## Title

PREPARATIVE AND STRUCTURAL STUDIES INVOLVING NOBLE-GAS AND RELATED COMPOUNDS.



## Author

McKee, Douglas Edward.

## Publication Date

1973-05-01

Thesis/dissertation

LBL-1814

# PREPARATIVE AND STRUCTURAL STUDIES INVOLVING NOBLE-GAS AND RELATED COMPOUNDS

Douglas Edward McKee
(Ph.D. Thesis)



May 1973

Prepared for the U. S. Atomic Energy Commission
under Contract W-7405-ENG-48



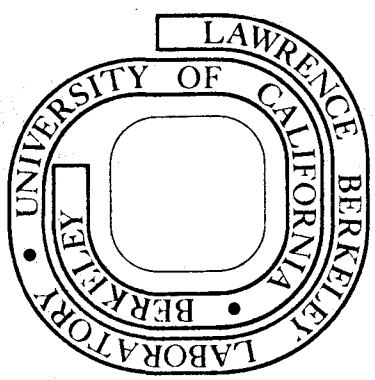


LBL-1814

## DISCLAIMER

to my parents, who have put up with a lot

I shall not forget

Table of Contents

# PREPARATIVE AND STRUCTURAL STUDIES INVOLVING NOBLE-GAS AND RELATED COMPOUNDS

Douglas Edward McKee

Inorganic Materials Research Division, Lawrence Berkeley Laboratory,
and Department of Chemistry; University of California
Berkeley, California 94720

## ABSTRACT

Several noble-gas cations were synthesized and characterized by vibrational spectroscopic and X-ray diffraction techniques. The complex $KrF_2 \cdot 2SbF_5$ was shown to be the salt $KrF^+Sb_2F_{11}^-$. This salt proved to be a powerful oxidizer, oxidizing $IF_5$ to $IF_6^+$ and $XeOF_4$ to $XeOF_5^+$. Reactions of $KrF^+Sb_2F_{11}^-$ with $BrF_5$ and $ClF_5$ are described. The $XeF_4$,$SbF_5$ system was studied, revealing the salts $XeF_3^+Sb_2F_{11}^-$ and $XeF_3^+SbF_6^-$. The latter salt was shown to be dimorphic with a transition temperature of ca. 95°. The X-ray crystal structure of $XeF_3^+Sb_2F_{11}^-$ was determined; the novel $XeF_3^+$ is T-shaped and is structurally similar to $BrF_3$ and $ClF_3$, its isoelectronic relatives. The bonding in the xenon fluoro-cations is discussed. In the $XeOF_4$,$SbF_5$ system, two salts were prepared and identified: $XeOF_3^+Sb_2F_{11}^-$ and $XeOF_3^+SbF_6^-$.

The salts $O_2^+Sb_2F_{11}^-$ and $O_2^+SbF_6^-$ were unambiguously characterized by vibrational spectroscopy and X-ray powder diffraction photography. Their convenient laboratory syntheses are described.

The oxidation of xenon by $IF_7$ at 280° to $XeF_2 \cdot IF_5$ is described. The thermodynamics of that and related reactions are discussed.

# I. INTRODUCTION

The work described in this thesis is organized by projects, in that each chapter is a discrete work. There are, however, many procedures and techniques, common to fluorine chemistry in general, which were applied to all of the thesis material. To avoid repetition, this chapter describes those common techniques; special procedures or apparatus peculiar to one or another of the individual projects are described in the appropriate chapters.

Chapter VI describes the chemistry of krypton (II), which is the most novel work of this thesis. The object of these experiments was to exploit the remarkable oxidizing potential of $Kr^{II}$ to synthesize new and interesting molecules. Characterizations of the $O_2^+$ salts derived from $SbF_5$ (Chapter II) and $XeF_3^+$ and $XeOF_3^+$ salts (Chapters III and IV), although of structural and bonding interest, provided information necessary for the interpretation of the krypton experiments, and were done primarily for that purpose. The work of Chapter V is unrelated to that of Chapter VI; it was done for the thermodynamic interest surrounding the oxidation of xenon.

## A. General Apparatus

Because of the air-sensitive nature of all of the compounds described, their handling required meticulous care. Non-volatile solids were manipulated under nitrogen in a Vacuum Atmosphers Dri-Lab, purged of water and oxygen by a continuously flowing circulation system. Regeneration of

the drying system was performed regularly as necessitated by frequent use of the box. Special attention was given to the gloves; they were replaced if cracked or flaking. The handling of volatile compounds, manipulation of solvents, and the carrying out of reactions were done on a metal vacuum system. The form of the system has been described elsewhere.[1] The materials in regular use were Monel and copper tubing, Monel and brass Whitey valves, and Monel Autoclave valves. A number of reactions were carried out in small, auxiliary Pyrex systems, specially fabricated for each experiment, and attached by Kovar-to-Pyrex seals to the metal vacuum system. Since it is relatively inert to oxidizers, Kel-F was used on valve tips and reaction vessels. Working pressures in the systems were provided by Monel Bourdon gauges. Pressures below 1 torr were determined using thermocouple and ion gauges, so placed that they could be isolated and protected from corrosive compounds. The mechanical and oil diffusion pumps were protected by large shut-off valves and liquid nitrogen traps. Periodic maintenance on the system was required. Because of attack on the metal, the tubing occasionally became clogged. Valve seats and stems were the most vulnerable parts of the system; the most frequently used valves often needed stem replacement. The entire vacuum system was housed in a large fume hood provided with a powerful exhaust fan.

Assurance of a leak-tight apparatus was of the utmost importance for dependable work. Leaks in the vacuum system were detected with the aid of a Consolidated Vacuum helium leak detector. All reaction vessels and auxiliary reaction systems were checked with the leak detector prior to each use.

## B. Routine Identification of Materials

### 1. Raman Spectroscopy

The most common method of identification of the compounds was Raman spectroscopy. The technique was employed routinely to check reactants prior to use and reaction products, and in general, as a "fingerprinting" device. A Cary 83 Spectrometer was used in this way. For precise data in identifying new compounds and for the most sophisticated information in characterization, the research instrument at the USDA Western Regional Laboratories in Albany was used. The instrument utilizes a Spex 1401 monochromator and photon counting techniques. The data can be digitized and stored directly on disk in the laboratory's IBM 1800 computer, which allows it to be intensity corrected for the phototube sensitivity, normalized, and plotted. The earliest spectra were obtained with excitation from a He-Ne laser (6328 Å, 100 mw). The majority of the spectra, however, were excited by $Ar^+$ and $Kr^+$ lasers (4880 Å, 1.5 w; 5145 Å, 1.5 w; 6471 Å, 400 mw), the line and power used depending on the color and sensitivity of the compound. All of the spectra appearing here were recorded with a monochromator slit width of 2 $cm^{-1}$. The resolution obtained by the scanning technique was 2 $cm^{-1}$. Samples were sealed in 1 mm quartz capillaries.

### 2. Infrared Spectroscopy

Infrared spectra were routinely recorded on a Perkin-Elmer 237 spectrometer in the range 400-4000 $cm^{-1}$. A Monel cell with AgCl windows

was used for gases. Solids were finely powdered and dusted onto AgCl plates sandwiched in a leak-tight Kel-F holder.

3. X-ray Powder Photography

A powder diffraction pattern was obtained for each solid material, to provide a purity criterion, to "fingerprint" the material, and to check that selected crystals were representative of the bulk material from which they came. In the usual technique samples were sealed in dried 0.3-0.5 mm O.D., .01 mm walled quartz capillaries on a G. E. Precision Camera, using graphite monochromatized Cu Kα radiation.

## II. THE DIOXYGENYL SALTS $O_2^+SbF_6^-$ AND $O_2^+Sb_2F_{11}^-$ AND THEIR CONVENIENT LABORATORY SYNTHESES

### A. History and Discussion

The first claim for the salt of formulation $O_2^+SbF_6^-$ was that of Young, *et al.*[2] These authors prepared their material by interaction of $O_2F_2$ with $SbF_5$. A puzzling feature of this report, however, was the rather large cubic unit cell quoted, for which a = 10.71 Å, since in the previously characterized[3] platinum analogue, a = 10.032 Å. In later papers Shamir and Binenboym described[4] a photochemical synthesis for what was claimed to be $O_2^+SbF_6^-$, and Beal, *et al.* described[5] a preparation from $SbF_5$, $F_2$, and $O_2$ which simply involved heating this mixture. The first authors presented no unambiguous evidence for the formulation $O_2^+SbF_6^-$, and quoted a cubic unit cell constant of 10.30 Å, a value which, although more acceptable than that of Young, *et al.*, still seemed rather high. Beal, *et al.* provided X-ray powder data to support a unit cell of 10.13 Å, a value in much closer harmony with the cell parameter for the cubic $O_2^+PtF_6^-$ salt.[3] The X-ray powder data of Beal, *et al.* was, however, ascribed to a face-centered cell, whereas the full data (some of which was omitted from their tabulation) supported a body-centered cell with a = 10.13 Å. It is now clear that weak diffraction lines were omitted from their data. These represented (as discussed[3] by Bartlett and Lohmann for the $O_2^+PtF_6^-$ case) diffraction by the light atom superlattice and are of crucial structural importance.

In their differential thermal analysis of $O_2^+SbF_6^-$ Nikitina and Rosolovskii recognized[6] the existence of the $O_2^+Sb_2F_{11}^-$ salt as well as

$O_2^+SbF_6^-$ and attempted a characterization of the two salts on the basis of X-ray powder data. Their data, however, is not that for the pure components $O_2^+SbF_6^-$ and $O_2^+Sb_2F_{11}^-$. Furthermore, Nikitina and Rosolovskii also failed to recognize $O_2^+SbF_6^-$ as an isomorph of $O_2^+PtF_6^-$.

Although the $O_2^+$ stretching frequency has been reported[7] for what was stated to be the $O_2^+SbF_6^-$ salt, the anion spectra were not given.

The X-ray powder data given in Table I and the Raman spectrum shown in Fig. 1b characterize the $O_2^+SbF_6^-$ salt. The X-ray data establish that the compound is isomorphous with $O_2^+PtF_6^-$. The unit cell is cubic with $a = 10.132\ 0.002$ Å, $V = 1040$ Å$^3$, $z = 8$, $\underline{D}_{\underline{C}} = 3.418$ g cm$^{-3}$. Since all observed reflections obey the conditions $\underline{h}+\underline{k}+\underline{\ell} = 2n$ and $\underline{0k\ell}$ : $\underline{k}(\underline{\ell}) = 2n$, the indicated space group is $\underline{Ia3}$ (#206)[8] as established for $O_2PtF_6$.[3,9] The formula unit volume of 130 Å$^3$ is 2.4 Å$^3$ less than that found for $NO^+SbF_6^-$ by Bartlett and Jha.[10] This is comparable to the $PtF_6^-$ case where $V(NO^+PtF_6^-) = 129.5$ Å$^3$ and $V(O_2^+PtF_6^-) = 126.3$ Å$^3$. The close similarity of the intensities of the weak powder diffraction lines (oxygen and fluorine diffraction only), compared with those in the platinum relative,[10] suggest an isostructural relationship. Comparison of the Raman spectrum with that of $O_2^+PtF_6^-$ (given in Fig. 1c) further supports the close structural similarity.

The X-ray powder data for $O_2^+Sb_2F_{11}^-$ given in Table II have not been indexed and all attempts to grow single crystals have failed. The Raman spectrum given in Fig. 1a again gives clear evidence of the $O_2^+$ ion (in the band at 1865 cm$^{-1}$) and the anion spectrum shows relationship to the $SbF_6^-$ spectrum. The anion spectrum is in fact simpler than in $XeF^+Sb_2F_{11}^-$ (ref. 12) and $XeF_3^+Sb_2F_{11}^-$ (ref. 13).

It may be that the anion in $O_2^+Sb_2F_{11}^-$ possesses a linear bridge and that the $O_2^+$ species are symmetrically placed about the anion. This would account for the absence of features in the Raman spectrum attributable to bridge stretching. In the $XeF^+Sb_2F_{11}^-$ and $XeF_3^+Sb_2F_{11}^-$ salts the bridge angles are 150° (ref. 14) and 155° (ref. 15), respectively, and the salts show Raman bands attributable to bridge stretch at 482 (ref. 12) and 487 $cm^{-1}$ (ref. 13), respectively. In $BrF_4^+Sb_2F_{11}^-$ where the bridge angle is not significantly deviant from linearity,[16] this Raman feature is not observed.[13] The presence of a band at 470 $cm^{-1}$ in the infrared spectrum of $O_2^+Sb_2F_{11}^-$ indicates that the strength of the bridge bond on the anion is not much different from that in the other salts, and coupled with the absence of its counterpart in the Raman, argues for a linear anion.

## B. Experimental

$O_2^+Sb_2F_{11}^-$ was prepared by irradiation of a fluorine, oxygen, and antimony pentafluoride mixture contained in a Pyrex bulb provided with a Kel-F tipped Whitey valve joined to the bulb through a Kovar seal. A 450 watt Hanovia ultraviolet lamp was used at a distance of 6 inches; irradiations lasted 12-16 hours.* A stoichiometry appropriate for the reaction $O_2 + \frac{1}{2}F_2 + 2SbF_5 \rightarrow O_2Sb_2F_{11}$ was found to be best; thus 69.0 mmoles $SbF_5$ with 34.5 mmoles $O_2$ and 17.3 mmoles $F_2$ in a 5 liter flask were quantitatively converted to $O_2Sb_2F_{11}$ in 12 hours. In irradiations where an excess of $F_2$ and $O_2$ over that required for $O_2Sb_2F_{11}$ formation prevailed, $O_2^+SbF_6^-$ was also observed in the product. Use of excess $SbF_5$

* The u.v. radiation reaching the reactants was cut off below 2800 Å by the Pyrex bulb.

necessitated the removal of this material from the product but this approach does provide pure $O_2^+Sb_2F_{11}^-$.

$O_2SbF_6$ was prepared by heating $O_2Sb_2F_{11}$ in a dynamic vacuum at 110°. At that temperature, the $SbF_5$ is removed slowly and at an approximately constant rate. If removal of $SbF_5$ is halted at a weight corresponding to loss of one mole of $SbF_5$ per mole of $O_2Sb_2F_{11}$, the material which remains provides the X-ray powder pattern and the Raman spectrum assigned to $O_2^+SbF_6^-$. The $O_2^+SbF_6^-$ salt itself is unstable under those preparative conditions, but $O_2^+Sb_2F_{11}^-$ decomposes to $O_2^+SbF_6^-$ at a greater rate. It is therefore essential to monitor the rate of loss of $SbF_5$ so that $SbF_5$ removal may be halted when the last of the $Sb_2F_{11}^-$ salt has decomposed. The conversion of 5.55 mmoles $O_2Sb_2F_{11}$ to 5.54 mmoles $O_2SbF_6$ required 282 hours at 110°. $O_2Sb_2F_{11}$ may be converted to $O_2SbF_6$ more rapidly under vacuum at higher temperatures, but the yield is lower; e.g., at 160° the conversion of 0.76 mmoles $O_2Sb_2F_{11}$ to 0.49 mmoles $O_2SbF_6$ was complete in only 3 hrs., the loss of material being due to thermal decomposition. X-ray powder photography and Raman spectroscopy revealed that removal of $SbF_5$ from $O_2^+Sb_2F_{11}^-$ was associated with the appearance of $O_2^+SbF_6^-$. No phases other than $O_2^+SbF_6^-$ and $O_2^+Sb_2F_{11}^-$ were indicated.

$O_2Sb_2F_{11}$ was also prepared from $O_2SbF_6$. The 1:1 salt (1.75 mmole) was placed in a Pyrex tube with excess $SbF_5$ (2-3 ml), under 300 mm of nitrogen pressure. The tube was brought to 125° and shaken. A clear solution was not obtained, but care was taken to break up the clumps of solid by agitating the mixture to a white slurry. The mixture was cooled

to room temperature before unreacted $SbF_5$ was removed under vacuum. The white solid which remained was shown by X-ray and Raman spectra to be $O_2Sb_2F_{11}$ and the weight corresponded to 1.61 mmoles.

The preparative technique for X-ray powder diffraction and Raman samples has been previously described.[13] Long exposure times were required to obtain a suitable powder pattern for $O_2^+Sb_2F_{11}^-$, but the 26 lines reported in Table II unambiguously fingerprint that compound. The Raman spectra have been intensity corrected for non-linear sensitivity of the phototube. For the antimony salts the exciting line was the 5145 Å $Ar^+$ line and for the deep red platinum salt, the 6741 Å $Kr^+$ line.

Infrared spectra from 4000-400 $cm^{-1}$ were recorded for both $O_2SbF_6$ and $O_2Sb_2F_{11}$. $O_2SbF_6$ shows only one broad band in the region examined, at 660-670 $cm^{-1}$, characteristic of the $\nu_3$ mode of the $SbF_6^-$ ion. $O_2Sb_2F_{11}$ shows three bands, centered at 677, 652, and 470 $cm^{-1}$.

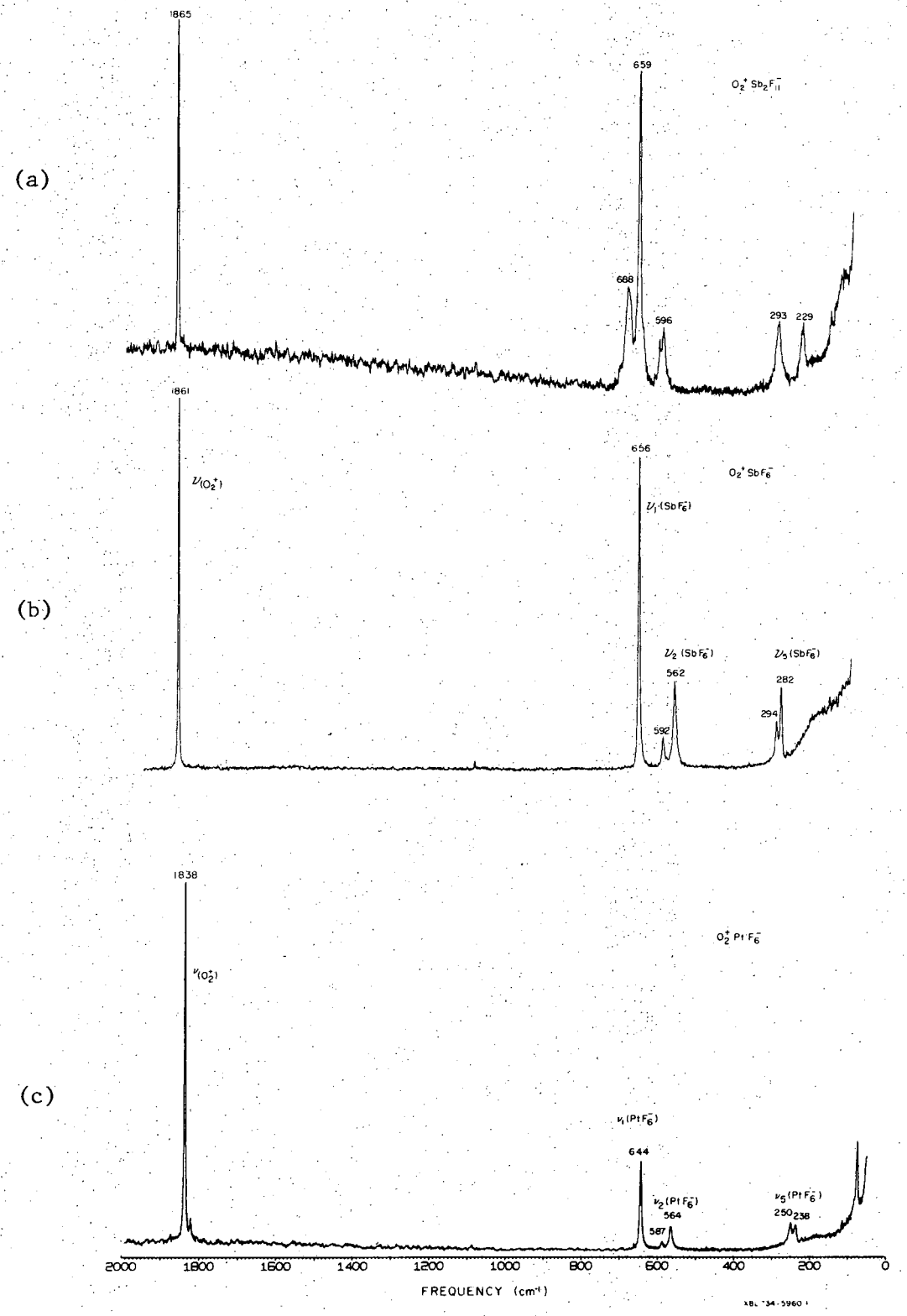


Figure II-1

Raman spectra of: (a) $O_2^+Sb_2F_{11}^-$; (b) $O_2^+SbF_6^-$; (c) $O_2^+PtF_6^-$

Table II-1

X-Ray Powder Data for $O_2^+SbF_6^-$

(Cubic: $\underline{a}$ = 10.132 ± 0.002 Å*, $\underline{V}$ = 1040 Å$^3$, $\underline{z}$ = 8, $D_c$ = 3.418 g/cm$^3$, Space group $\underline{Ia\bar{3}}$, Cu Kα radiation Ni filter).

| dÅ | $1/d^2_{obs}$ | $1/d^2_{calc}$ | h k ℓ | $I/I_o$ |
|---|---|---|---|---|
| 5.091 | .0385 | .0390 | 2 0 0 | 8 |
| 3.595 | .0772 | .0779 | 2 2 0 | 10 |
| 2.915 | .1175 | .1169 | 2 2 2 | 5 |
| 2.697 | .1371 | .1364 | 3 2 1 | 2 |
| 2.534 | .1556 | .1558 | 4 0 0 | 4 |
| 2.389 | .1751 | .1753 | 4 1 1 | 2 |
| 2.260 | .1957 | .1948 | 4 2 0 | 5 |
| 2.159 | .2144 | .2143 | 3 3 2 | 3 |
| 2.067 | .2339 | .2338 | 4 2 2 | 7 |
| 1.980 | .2550 | .2533 | 4 3 1 | 1 |
| 1.785 | .3138 | .3117 | 4 4 0 | 5 |
| 1.685 | .3520 | .3507 | 4 4 2, 6 0 0 | 5 |
| 1.597 | .3919 | .3896 | 6 2 0 | 5 |
| 1.521 | .4322 | .4286 | 6 2 2 | 5 |
| 1.461 | .4685 | .4676 | 4 4 4 | 2 |
| 1.430 | .4891 | .4871 | 5 4 3 | < 1 |
| 1.401 | .5095 | .5065 | 6 4 0 | 4 |
| 1.374 | .5294 | .5260 | 7 2 1 | 1 |
| 1.351 | .5480 | .5455 | 6 4 2 | 5 |
| 1.283 | .6070 | .6040 | 7 3 2 | 1 |
| 1.265 | .6257 | .6234 | 8 0 0 | 1 |
| 1.226 | .6650 | .6624 | 8 2 0, 6 4 4 | 4 |

* Cell dimension obtained from an extrapolation using the Nelson-Riley function.[17]

Table II-1 (continued)

| dA | $1/d^2_{obs}$ | $1/d^2_{calc}$ | h k ℓ | $I/I_o$ |
|---|---|---|---|---|
| 1.192 | .7047 | .7014 | 8 2 2, 6 6 0 | 4 |
| 1.160 | .7435 | .7403 | 6 6 2 | 3 |
| 1.131 | .7827 | .7793 | 8 4 0 | 3 |
| 1.104 | .8212 | .8182 | 8 4 2 | 3 |
| 1.077 | .8623 | .8572 | 6 6 4 | 3 |
| 1.033 | .9371 | .9351 | 8 4 4 | 2 |
| 1.012 | .9759 | .9741 | 10, 0, 0; 8 6 0 | 2 |
| .9926 | 1.015 | 1.013 | 10, 2, 0; 8 6 2 | 4 |
| .9738 | 1.054 | 1.052 | 10, 2, 2; 6 6 6 | 3 |
| .9396 | 1.132 | 1.130 | 10, 4, 0; 8 6 4 | 4 |
| .9240 | 1.171 | 1.169 | 10, 4, 2 | 3 |
| .8945 | 1.249 | 1.247 | 8 8 0 | 1 |
| .8811 | 1.287 | 1.286 | 10, 4, 4; 8 8 2 | 3 |
| .8681 | 1.326 | 1.325 | 10, 6, 0; 8 6 6 | 3 |
| .8556 | 1.365 | 1.364 | 10, 6, 2 | 3 |
| .8438 | 1.404 | 1.403 | 12, 0, 0; 8 8 4 | 3 |
| .8324 | 1.443 | 1.442 | 12, 2, 0 | 2 |
| .8215 | 1.482 | 1.481 | 12, 2, 2; 10, 6, 4 | 4 |
| .8006 | 1.560 | 1.558 | 12, 4, 0 | 2 |
| .7910 | 1.598 | 1.597 | 12, 4, 2; 10, 8, 0; 8 8 6 | 6 |
| .7816 | 1.637 | 1.636 | 10, 8, 2 | 4 |

Table II-2

X-Ray Powder Data for $O_2^+Sb_2F_{11}^-$
(Cu-Kα radiation Ni filter)

| dA° | $1/d^2$ | $I/I_o$ |
|---|---|---|
| 7.809 | .0164 | 1 |
| 6.476 | .0238 | 1 |
| 5.739 | .0304 | 2 |
| 5.354 | .0349 | 6 (broad) |
| 4.941 | .0410 | 2 |
| 4.634 | .0465 | 1 |
| 4.306 | .0539 | 1 |
| 3.951 | .0640 | 10 (broad) |
| 3.767 | .0705 | 1 |
| 3.616 | .0765 | 6 (broad) |
| 3.436 | .0847 | 2 |
| 3.213 | .0969 | 1 (v. broad) |
| 2.948 | .1151 | 1 |
| 2.824 | .1253 | 3 |
| 2.721 | .1350 | 3 |
| 2.622 | .1453 | 2 |
| 2.520 | .1575 | 1 |
| 2.454 | .1661 | 3 |
| 2.131 | .2201 | 2 |
| 2.031 | .2423 | 2 |
| 1.949 | .2632 | 1 |
| 1.882 | .2822 | 1 |
| 1.791 | .3117 | 1 |

Table II-2 (continued)

| dÅ | $1/d^2$ | $I/I_o$ |
|---|---|---|
| 1.704 | .3442 | 1 |
| 1.651 | .3665 | 1 |
| 1.618 | .3822 | 3 |

# III. THE PREPARATION AND RAMAN SPECTRA OF THE SALTS $XeF_3^+SbF_6^-$, $XeF_3^+Sb_2F_{11}^-$, $XeOF_3^+SbF_6^-$, AND $XeOF_3^+Sb_2F_{11}^-$

## A. Introduction

Bartlett and Sladky[18] have presented evidence for a decrease in fluoride ion donor ability of the xenon fluorides in the sequence $XeF_6 > XeF_2 > XeF_4$. Indeed, since $XeF_2$ and $XeF_6$ form complexes with $RuF_5$ and $AsF_5$, whereas $XeF_4$ does not, this provides for the chemical purification of the tetrafluoride. The X-ray crystal structures of these complexes indicate the salt formulations: $Xe_2F_3^+AsF_6^-$ (ref. 19) and $XeF_5^+AsF_6^-$ (ref. 20), $XeF^+RuF_6^-$ and $XeF_5^+RuF_6^-$ (ref. 21). It remained to establish, however, that $XeF_4$ could behave as a fluoride ion donor. It was known from early work[22] that $XeF_4$ was capable of complexing with the best fluoride ion acceptor, $SbF_5$. More recently, Martin[23] claimed 2:1 and 1:4 complexes but adequate characterization was lacking. It seemed that a similar variety of complexes might occur in the $XeF_4/SbF_5$ system as had been established for the $XeF_2/MF_5$ (ref. 24) and $XeF_6/MF_5$ (ref. 25) systems. Furthermore, since a characterization of the $XeOF_4/SbF_5$ system was necessary for the work in Chapter VI, and the $XeF_4$ molecule has a simple relationship to $XeOF_4$, a parallel study with that compound was undertaken. Selig had established[26] a complex $XeOF_4 \cdot 2SbF_5$, but structural information was not given.

Since the onset of this study, Gillespie *et al.*[27] have provided $^{19}F$ n.m.r. structural information and vibrational spectroscopic evidence for the salt $XeF_3^+Sb_2F_{11}^-$. Our vibrational spectroscopic findings are

in substantial agreement with theirs, and the crystallographic findings described in the next chapter establish the salt formulation. This work also establishes the salt $XeF_3^+SbF_6^-$. Two complexes have been identified in the $XeOF_4/SbF_5$ system and are formulated as $XeOF_3^+SbF_6^-$ and $XeOF_3^+-Sb_2F_{11}^-$. The last has been described in a recent note[28] by Gillespie and his coworkers.

## B. Experimental

Reagents. Xenon tetrafluoride was prepared by the method of Claassen, Selig and Malm.[29] It was purified by melting in a Kel-F tube with ruthenium pentafluoride or arsenic pentafluoride, after the procedure given by Bartlett and Sladky.[18] The high purity of each batch was established by Raman spectroscopy and melting point (117°). Xenon oxide tetrafluoride was prepared by the interaction of $XeF_6$ with quartz at 50°.[30] It was essential, for safety and effectiveness, to immerse the entire bulb up to the enclosing valve, in the water bath. Before the characteristic yellow color of $XeF_6$ had completely disappeared, the contents of the quartz bulb were transferred under vacuum to a Kel-F trap containing sodium fluoride. (CAUTION: If all of the $XeF_6$ is consumed, $XeO_3$ may form and detonate.) $SiF_4$ was removed under vacuum at -78°. The mixture in the trap was heated to 50° to convert remaining $XeF_6$ to the $NaF-XeF_6$ complex.[31] Finally, $XeOF_4$ was separated by vacuum distillation at room temperature to traps at -196°. Infrared spectroscopy showed only those bands characteristic of $XeOF_4$ (ref. 32). Antimony pentafluoride was prepared from the oxide by fluorination[33]

in an inclined Pyrex tube and purified by trap-to-trap distillation in a dynamic vacuum.

Complexes. The complexes of $XeOF_4$ and of $XeF_4$ with $SbF_5$ were prepared from their components as detailed below. The components were mixed in a variety of known molar ratios and each composition was characterized by Raman, X-ray powder and (occasionally) single crystal data. These studies indicated that compounds exist with the following compositions: $XeF_4 \cdot SbF_5$; $XeF_4 \cdot 2SbF_5$; $XeOF_4 \cdot SbF_5$; and $XeOF_4 \cdot 2SbF_5$.

$XeOF_4 \cdot 2SbF_5$ (m.p. 61-65°) was prepared by distilling a known weight of $XeOF_4$ into a quartz trap, followed by an excess of $SbF_5$. The trap was heated until solution was complete, then cooled to room temperature, at which point the excess $SbF_5$ was removed by vacuum distillation. A colorless solid remained.

$XeOF_4 \cdot SbF_5$ (m.p. 104-105°) was prepared by distilling excess $XeOF_4$ onto a known weight of $XeOF_4 \cdot 2SbF_5$ in a quartz trap, which was gently heated to complete solution. Excess $XeOF_4$ was removed by vacuum distillation and yielded a colorless solid.

$XeF_4 \cdot 2SbF_5$ (m.p. 81-83°) was prepared similarly to $XeOF_4 \cdot 2SbF_5$. The solid was pale yellow-green.

$XeF_4 \cdot SbF_5$ (m.p. 109-113°) was derived from the 1:2 compound by combining equimolar quantities of $XeF_4$ and $XeF_4 \cdot 2SbF_5$. The compounds were placed in a Pyrex tube closed with a Kel-F tipped Whitey valve, #1KS4. The mixture was heated under dry nitrogen until a homogeneous melt was obtained. The melt was allowed to cool slowly to room temperature.

$XeF_4 \cdot SbF_5$ was also prepared by directly combining and melting together equimolar quantities of $XeF_4$ and $SbF_5$. The solid was pale yellow-green. It proved to be dimorphic, with a transition temperature of ~95°. Each form provides a distinctive Raman spectrum (Table III-1). At room temperature the transition to the low temperature form required 2-3 days.

Crystal Data. Single crystals of $XeF_4 \cdot SbF_5$ (low temperature form) were obtained by slow removal of the solvent, at -10°, from a solution in anhydrous HF. Found: Monoclinic, $\underline{a}$ = 5.50, $\underline{b}$ = 15.50, $\underline{c}$ = 8.945 (all ±0.01 Å), $\beta$ = 102.9±.3°, $\underline{V}$ = 743.3 Å$^3$, $\underline{z}$ = 4, $\underline{D}_c$ = 3.81 g cm$^{-3}$.

Excess $XeF_4$ in fused admixture with $XeF_4 \cdot SbF_5$, failed to produce compounds richer in $XeF_4$.

## C. Results and Discussion

As well as providing distinctive fingerprints for the compounds detected in the $XeF_4/SbF_5$ and $XeOF_4/SbF_5$ systems, Raman spectroscopy afforded information about the nature of the species present. In no case do the spectra of the solids show the characteristic Raman lines of the parent molecular fluorides;[13] by the same token, neither $XeF_4$ nor $XeOF_4$ is present as such in antimony pentafluoride solution, at least in amounts detectable by the Raman effect. The spectra are consistent, however, with the expected ionic structures containing $XeF_3^+$ or $XeOF_3^+$ cations; the crystallographic study of $XeF_4 \cdot 2SbF_5$ (shown to be $XeF_3^+Sb_2F_{11}^-$) described in the following chapter confirmed this expectation, and provided a fixed point in the interpretation of the spectroscopic

data. A further aid in this task, and in assigning frequencies, was Raman data, either obtained in this laboratory or gleaned from the literature, for antimony pentafluoride adducts of other fluoride-ion donors (see footnotes in Table III-1).

The problem of identifying cation and anion bands in the $XeF_4/SbF_5$ and $XeOF_4/SbF_5$ systems is by no means straightforward. Both cation and anion stretching fundamentals occur in the same region of the spectrum (450-750 $cm^{-1}$), while comparison with other compounds of this sort shows no truly characteristic spectroscopic pattern for either $SbF_6^-$ or $Sb_2F_{11}^-$; the former anion commonly suffers severe distortions from $O_h$ symmetry. Nevertheless, the solids and solutions examined displayed apt and consistent sets of Raman lines attributable to $XeF_3^+$ or $XeOF_3^+$ cations. Further encouragement in this set of assignments was the comparison of these frequencies with the corresponding fundamentals of related molecules derived from a trigonal bipyramidal unit (Table III-6). The gist of the arguments which led to what seems to be the most reasonable set of assignments is given in the following paragraphs.

Like the monomeric halogen trifluoride molecules,[34] the T-shaped $XeF_3^+$ cation has essentially $C_{2v}$ symmetry, and should display two strong, polarized Raman lines in the region associated with Xe-F stretching fundamentals. These lines are indeed observed at ca. 640 $cm^{-1}$ and ca. 575 $cm^{-1}$, and are assigned respectively to $\nu_1(a_1)$, involving principally the equatorial Xe-F bond, and $\nu_2(a_1)$, associated with the symmetric stretching motion of the axial $XeF_2$ unit. The antisymmetric stretching fundamental of the $XeF_2$ unit, $\nu_4(b_1)$, is normally only weakly Raman

active, and is expected to lie at slightly higher frequency than $\nu_2(a_1)$ ($BrF_3$: $\nu_2(a_1)$ 552 $cm^{-1}$, $\nu_4(b_1)$ 612 $cm^{-1}$ (ref. 34); see also Table III-6); this fundamental is not observed for $XeF_3^+$ in solution in antimony pentafluoride, but is identified with weak lines at ca. 614 $cm^{-1}$ in the spectra of $XeF_4 \cdot SbF_5$ and $XeF_4 \cdot 2SbF_5$. A line at ca. 360 $cm^{-1}$ is attributed to a deformation of the axial $XeF_2$ group. Some of the $XeF_3^+$ fundamentals occur as doublets in the room temperature modification of $XeF_3^+SbF_6^-$; a similar effect is noted for $XeOF_3^+SbF_6^-$, and also for $IF_4^+SbF_6^-$ (ref. 35).

The $XeOF_3^+$ cation is expected to be structurally akin to $XeF_3^+$, with the oxygen atom of the former situated at one of the equatorial-lone-pair sites of the latter. A polarized Raman line at ca. 940 $cm^{-1}$ is approximately situated for an Xe-O stretching vibration, and the pattern of Xe-F stretches seen for $XeOF_3^+$ is remarkably like that of $XeF_3^+$. Polarized Raman lines occur at ca. 640 $cm^{-1}$ and ca. 590 $cm^{-1}$ (cf. $XeF_3^+$ 640, 575 $cm^{-1}$), and are assigned like their $XeF_3^+$ counterparts, to the equatorial Xe-F and symmetric axial $XeF_2$ stretching motions respectively. Unlike Gillespie *et al.*[28] who attributed Raman lines at ca. 550 $cm^{-1}$ in $XeOF_3^+Sb_2F_{11}^-$ to the antisymmetric stretching motion of the axial $XeF_2$ unit, we prefer to assign this fundamental above 600 $cm^{-1}$, prompted both by the comparison with $XeF_3^+$ and the evidence of similar molecules which shows the antisymmetric stretch to lie higher than its symmetric counterpart.

The vibrational data for the $XeF_3^+$ and $XeOF_3^+$ cations are not sufficiently complete to allow worthwhile normal coordinate analysis; the approximations necessary would be too severe. Nevertheless, if the

assignments for the $XeF_3^+$ and $XeOF_3^+$ vibrational modes and the suppositions concerning the $XeOF_3^+$ shape are valid, the bond lengths in $XeOF_3^+$ can be predicted with fair precision. Since the stretching frequency $\nu$(Xe-O) is not very different for the cation (939 $cm^{-1}$) compared with the value in the parent molecule (923 $cm^{-1}$), it is probably safe to assume that the Xe-O bond lengths will be similar (XeO in $XeOF_4$ = 1.70(2) Å) (ref. 36). Moreover, the Xe-F distance will not differ greatly for the two cations (1.83 Å in $XeF_3^+$), although the higher axial stretching fundamentals found for the Xe(VI) cation imply that the axial Xe-F bonds in $XeOF_3^+$ may be slightly shorter than in $XeF_3^+$ (1.88, 1.89 Å).

It is of interest that no evidence for either $Xe_2F_7^+$ or $Xe_2O_2F_7^+$ was found in these studies, although both $Xe_2F_3^+$ (ref. 19) and $Xe_2F_{11}^+$ (ref. 37) have been established. This is consistent with $XeF_4$ and $XeOF_4$ being inferior $F^-$ ion donors compared with either $XeF_2$ or $XeF_6$. The complex cations, in effect, involve fluoride ion donation by the neutral molecule to its daughter cation.

Finally, it should be noted that $XeOF_4$ and $IF_5$ are extremely similar in their fluoro-acid-base chemistry. Both form 1:1 and 1:2 adducts with the $F^-$ acceptor $SbF_5$, for which ionic formulations are appropriate, $XeF_3^+SbF_6^-$, $XeF_3^+Sb_2F_{11}^-$, $IF_4^+SbF_6^-$ (ref. 35), $IF_4^+Sb_2F_{11}^-$ (ref. 38). Molecular adducts, $XeF_2 \cdot XeOF_4$ (ref. 39) and $XeF_2 \cdot IF_5$ (ref. 40) are given with xenon difluoride while cesium fluoride affords both 1:1 and 1:3 complexes with $XeOF_4$ (see below) and with $IF_5$ (ref. 41).

## Appendix

In order to study further the similar chemical behavior of $IF_5$ and $XeOF_4$, the interaction of CsF and $XeOF_4$ was investigated. A known weight of finely divided CsF was placed in a quartz trap arrangement equipped with Kel-F tipped Whitey valve. 2-3 ml of $XeOF_4$ was distilled into the trap at -196° and allowed to warm and run onto the CsF. Reaction (bubbling and mist formation) was observed at initial contact. A colorless solid of volume greater than the original CsF was present which was insoluble in the $XeOF_4$ at room temperature. When the trap was pumped to constant weight, the solid remaining corresponded to $CsF \cdot 1.05\ XeOF_4$. In a second experiment, a weight vs. time curve revealed the existence of a compound of composition $CsF \cdot 3XeOF_4$, but there was no break in the curve at 1:2. In a separate experiment, removal of the $XeOF_4$ under vacuum was halted at the 1:3 composition, and a Raman spectrum and X-ray powder pattern demonstrated the existence of a phase of that composition, distinct from $CsF \cdot XeOF_4$. The lowering of the Xe-F and Xe=O stretching frequencies in the Raman spectra of these compounds (Fig. III-2) is consistent with the ionic formulations $Cs^+XeOF_5^-$ and $Cs^+Xe_3O_3F_{13}^-$. The powder data for both compounds are presented in Table III-7.

## Table III-1 Raman Frequencies for the $XeF_3^+$ and $XeOF_3^+$ Salts

| $XeF_3^+$ in $SbF_5$ | $XeF_3^+Sb_2F_{11}^-$ | $XeF_3^+SbF_6^-$ (h.t.) | $XeF_3^+SbF_6^-$ (l.t) | $XeOF_3^+$ in $SbF_5$ | $XeOF_3^+Sb_2F_{11}^-$ | $XeOF_3^+SbF_6^-$ | |
|---|---|---|---|---|---|---|---|
| **Cation stretching features** | | | | | | | |
| | | | | 939 p | 947(68) | 948(80) | $\nu$(Xe=O) |
| 642 p | 643(75) | 647(100) | 656(36)<br>649(59) | 642 p | 635(72) | 634(68) | $\nu$(Xe-$F_{eq}$) |
| | 618(sh) | 615(9) | 605(19) | | 643(65) | 624(40) | $\nu_{asymm}$(Xe-$F_2$(ax)) |
| 584 p | 585(100) | 571(92) | 580(95)<br>567(95) | 597 p | 596(100) | 589(sh)<br>583(100) | $\nu_{symm}$(Xe-$F_2$(ax)) |
| **Other features** | | | | | | | |
| (a) | (c) | (b) | (b) | (a) | (c) | (b) | |
| | 719(5) | | | | 712(35) | | |
| | 705(17) | 691(27) | 694(7) | | 705(27) | 696(33) | |
| | 684(44) | | | | 692(19) | 686(17) | |
| | 671(35) | 670(5) | 667(100) | | 667(sh) | 667(17) | |
| | 634(51) | 655(30) | 630(67) | | 621(20) | 660(16) | $\nu$(Sb-F) |
| | 553(31) | 583(sh) | 518(30) | | 559(25) | 549(24) | |
| | 493(4) | 455(19) | | | 538(20) | 507(17) | |
| | 365(11) | | 365(14) | | 356(18) | 367(13) | $\delta$(O=Xe-F) and |
| | | | | | 340(17) | 348(9) | $\delta$(F-Xe-F) |
| | | | | | | 338(14) | |
| | 305(12) | 297(10) | 322(8) | | 323(27) | 328(18) | |
| | 285(10) | 289(12) | 303(16) | | 296(21) | 283(15) | $\delta$(F-Xe-F) and |
| | 270(12) | 275(12) | 293(18) | | 265(21) | | $\delta$(F-Sb-F) |
| | 237(14) | | 276(26) | | 233(29) | 239(10) | |
| | 207(9) | 209(7) | | | | 209(12) | |

(a) Solvent and anion bands omitted.

(b) Raman lines for $SbF_6^-$: in $KSbF_6$(c); 661(vs), 575(s), 294(m), 278(m);
H. A. Carter and F. Aubke, Canad. J. Chem., 48 (1970) 3456;

in $IF_4^+SbF_6^-$; 694(7.2), 662(27.5), 570(7), 525(6), 299(4), 242(0+);
Reference 35.

in $Xe_2F_3^+SbF_6^-$; 660(2), 646(27), 572(10), 561(15), 517(1), 281(12);
R. Mews and N. Bartlett, to be published.

in $BrF_2^+SbF_6^-$; 686(9), 678(43), 661(1), 638(41), 547(35), 492(9), 281(7), 270(16);
K. O. Christe and C. J. Schack, Inorg. Chem. 9, 2296 (1970).

(c) Raman lines for $Sb_2F_{11}^-$: in $KrF^+Sb_2F_{11}^-$; 693(s), 679(m), 670(w), 651(s), 619(s), 521(m), 481(m), 298(w), 270(w), 230(w).
N. Bartlett and D. E. McKee, unpublished observations;

in $BrF_4^+Sb_2F_{11}^-$; 710(11), 705(11), 699(23), 687(5), 647(80), 588(8), 547(27), 296(11), 265(10), 238(13);
N. Bartlett, D. E. McKee and C. J. Adams, unpublished observations.

**Table III-2**

X-Ray Powder Data for $XeF_4 \cdot SbF_5$

(monoclinic: $\underline{a}$ = 5.50, $\underline{b}$ - 15.50, $\underline{c}$ = 8.945 Å, $\underline{\beta}$ = 102.9°

Space Group $\underline{P2_1/c}$)

| dÅ | $10^4\ 1/d^2_{obs}$ | $10^4\ 1/d^2_{calc}$ | h k ℓ | $I/I_o$ |
|---|---|---|---|---|
| 7.820 | 163 | 166 | 0 2 0 | mw |
| 4.999 | 400 | 403 | $\bar{1}$ 0 2 | w |
| 4.796 | 434 | 444 | $\bar{1}$ 1 2 | w |
| 4.333 | 532 | 532 | $\bar{1}$ 2 1 | s, broad |
| 4.120 | 589 | 591 | 0 1 2 | w |
| 3.926 | 648 | 646 | $\bar{1}$ 1 0 | ms |
| 3.744 | 713 | 716 | 0 2 2 | vw |
| 3.630 | 758 | 756 | $\bar{1}$ 1 3 | vw |
| 3.556 | 790 | 803 | 0 4 1 | ms |
| 3.386 | 872 | 881 | $\bar{1}$ 2 3 | s |

Table III-3

X-Ray Powder Data for $XeF_4 \cdot 2SbF_5$ (triclinic: $\underline{a}$ = 8.237, $\underline{b}$ = 9.984, $\underline{c}$ = 8.004, $\underline{\alpha}$ = 72.54, $\underline{\beta}$ = 112.59, $\underline{\gamma}$ = 117.05, Space Group = $P_T$)

| dÅ | $10^4\ 1/d^2_{obs}$ | $10^4\ 1/d^2_{calc}$ | h k ℓ | $I/I_o$ |
|---|---|---|---|---|
| 6.049 | 273 | 269 | 0 1 1 | w |
| | | 276 | $\bar{1}$ 0 1 | |
| 4.416 | 513 | 517 | 0 2 0 | s, broad |
| 4.065 | 605 | 604 | $\bar{2}$ 1 1 | w |
| 3.747 | 711 | 711 | 1 1 1 | s, broad |
| 3.513 | 808 | 812 | 2 0 0 | s |
| 3.365 | 883 | 891 | $\bar{2}$ 1 2 | m |
| 3.095 | 1043 | 1044 | $\bar{2}$ 3 1 | w |
| 2.910 | 1180 | 1180 | 1 0 2 | w |
| 2.619 | 1457 | 1457 | 0 $\bar{2}$ 2 | vw |
| 2.581 | 1500 | 1495 | 0 $\bar{3}$ 1 | vw |

Table III-4

X-Ray Powder Data for $XeOF_4 \cdot SbF_5$

| dÅ | $10^4$ $1/d^2$ | $I/I_o$ |
|---|---|---|
| 8.925 | 126 | w |
| 4.995 | 400 | m |
| 4.742 | 441 | vw |
| 4.459 | 502 | s |
| 4.281 | 545 | ms |
| 4.193 | 568 | w |
| 3.857 | 672 | w, broad |
| 3.681 | 738 | m |
| 3.576 | 782 | w |
| 3.440 | 844 | vw |

Table III-5

X-Ray Powder Data for $XeOF_4 \cdot 2SbF_5$

| dÅ | $10^4$ $1/d^2$ | $I/I_o$ |
|---|---|---|
| 7.394 | 183 | vvw |
| 4.490 | 494 | w |
| 4.305 | 539 | vw |
| 4.147 | 581 | m |
| 4.051 | 609 | m |
| 3.543 | 797 | w |
| 3.425 | 852 | w |
| 2.103 | 2261 | vw |
| 1.936 | 2667 | vw |

# Table III-6

## Raman frequencies for pseudo-trigonal bipyramidal molecules

| $XeF_2$[a] | $XeF_3^+$[b] | $XeOF_3^+$[b] | $IOF_3$[c,d] | $XeO_2F_2$[e] | $IF_4^+$[f] | $TeF_4$[g] | |
|---|---|---|---|---|---|---|---|
|  |  |  |  |  |  |  | |
| | | 939 | 878 | | | | $\nu$, E=O |
| | | | | 822 | | | $\nu_{symm}$, $EO_2$ |
| | | | | 850 | | | $\nu_{asym}$, $EO_2$ |
| | | | | | 733 | 695 | $\nu_{symm}$, eq. $EF_2$ |
| | | | | | 720 | 682 | $\nu_{asym}$, eq. $EF_2$ |
| | 640 | 642 | 651 | | | | $\nu$, eq. E-F |
| 557 | 618 | 649 | 545 | 585 | 645 | 588 | $\nu_{symm}$, ax $EF_2$ |
| 515 | 582 | 597 | 512 | 537 | 625<br>614 | 572 | $\nu_{asym}$, ax $EF_2$ |
| 213 | 363 | 358 | 351 | 324 | 389 | 333 | Deformation, $EF_2$ |

(a) Values for vapour-phase molecule: P. Tsao, C. C. Cobb, and H. H. Claassen, J. Chem. Phys. 54 5247 (1971); S. Reichman and F. Schreiner, ibid., 51 2355 (1969).

(b) This work.

(c) Reference 76.

(d) D. E. McKee and N. Bartlett, to be published.

(e) Reassignment of frequencies for matrix-isolated molecule reported by: H. H. Claassen, E. L. Gasner, and H. Kim, J. Chem. Phys. 49 253 (1968).

(f) Values for $IF_4^+SbF_6^-$(s); Reference 35.

(g) Values for matrix-isolated molecule; Reference 77.

Table III-7

A. X-Ray Powder Data for $CsF \cdot XeOF_4$

| d Å | $10^4$ $1/d^2$ | $I/I_o$ |
|---|---|---|
| 5.906 | 287 | 2 |
| 5.348 | 348 | 1 |
| 5.052 | 392 | 2 |
| 3.903 | 658 | 10 |
| 3.723 | 724 | 1 |
| 3.582 | 779 | 10 |
| 3.395 | 868 | 2 |
| 3.291 | 923 | 3 |
| 2.910 | 1181 | 1 |
| 2.705 | 1366 | 2 |
| 2.528 | 1564 | 2 |
| 2.441 | 1678 | 2 |
| 2.364 | 1789 | 2 |
| 2.557 | 1962 | 1 |
| 2.059 | 2358 | 6 |
| 1.971 | 2577 | 2 |
| 1.941 | 2653 | 3 |
| 1.856 | 2902 | 2 |
| 1.786 | 3135 | 4 |
| 1.724 | 3361 | 5 |
| 1.684 | 3527 | 2 |
| 1.598 | 3916 | 5 |
| 1.545 | 4187 | 1 |
| 1.522 | 4319 | 5 |
| 1.402 | 5086 | 3 |
| 1.350 | 5782 | 4 |
| 1.225 | 6663 | 4 |
| 1.191 | 6055 | 3 |

B. X-ray Powder Data for $CsF \cdot 3XeOF_4$

| d Å | $10^4$ $1/d^2$ | $I/I_o$ |
|---|---|---|
| 4.963 | 406 | 1 |
| 4.381 | 521 | 1 |
| 4.110 | 592 | 10 |
| 3.979 | 631 | 10 |
| 3.805 | 691 | 2 |
| 3.565 | 787 | 4 |
| 3.316 | 910 | 1 |
| 3.066 | 1064 | 5 |
| 2.888 | 1199 | 1 |
| 2.797 | 1278 | 1 |
| 2.649 | 1424 | 1 |
| 2.528 | 1564 | 4 |
| 2.217 | 2034 | 3 |
| 2.063 | 2350 | 4 |
| 1.988 | 2531 | 3 |
| 1.903 | 2761 | 2 |
| 1.856 | 2902 | 3 |

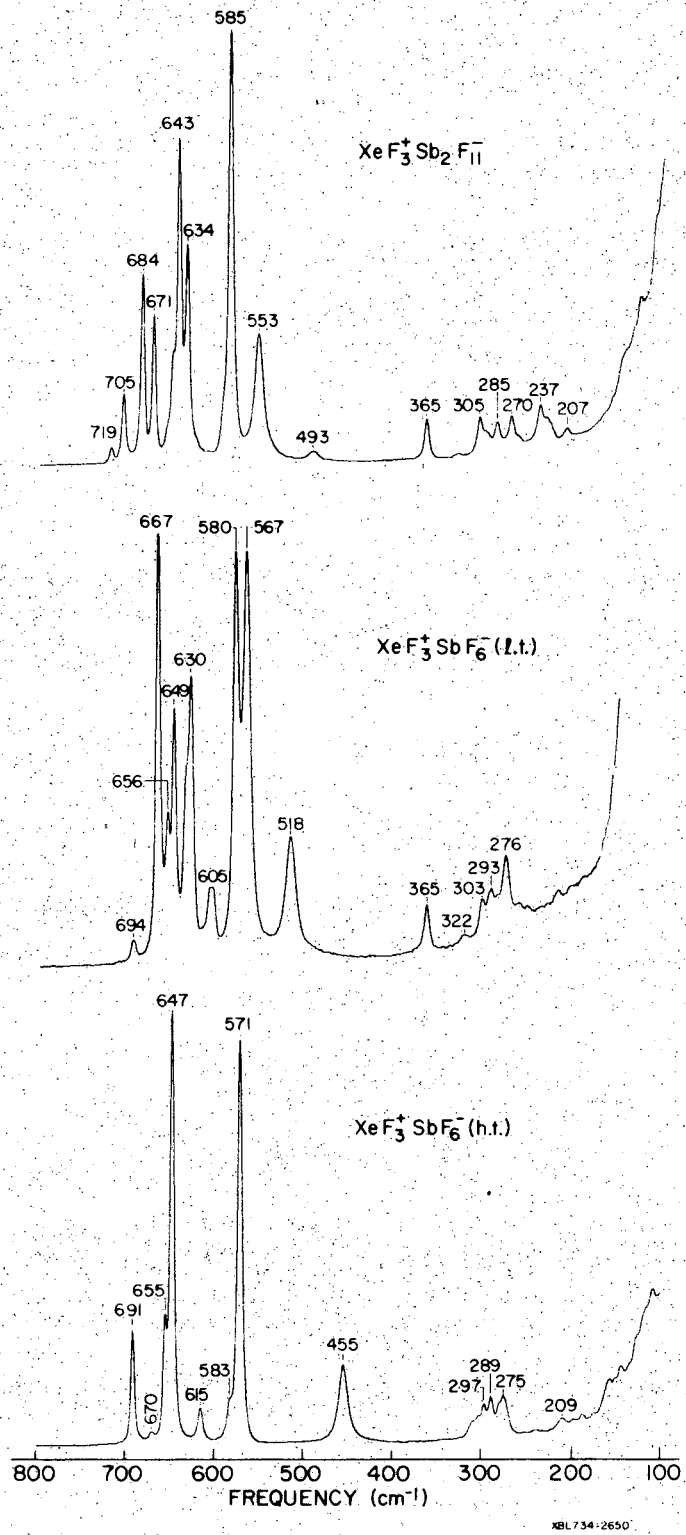


Figure III-1a Raman spectra of the $SbF_5$ salts of $XeF_4$.

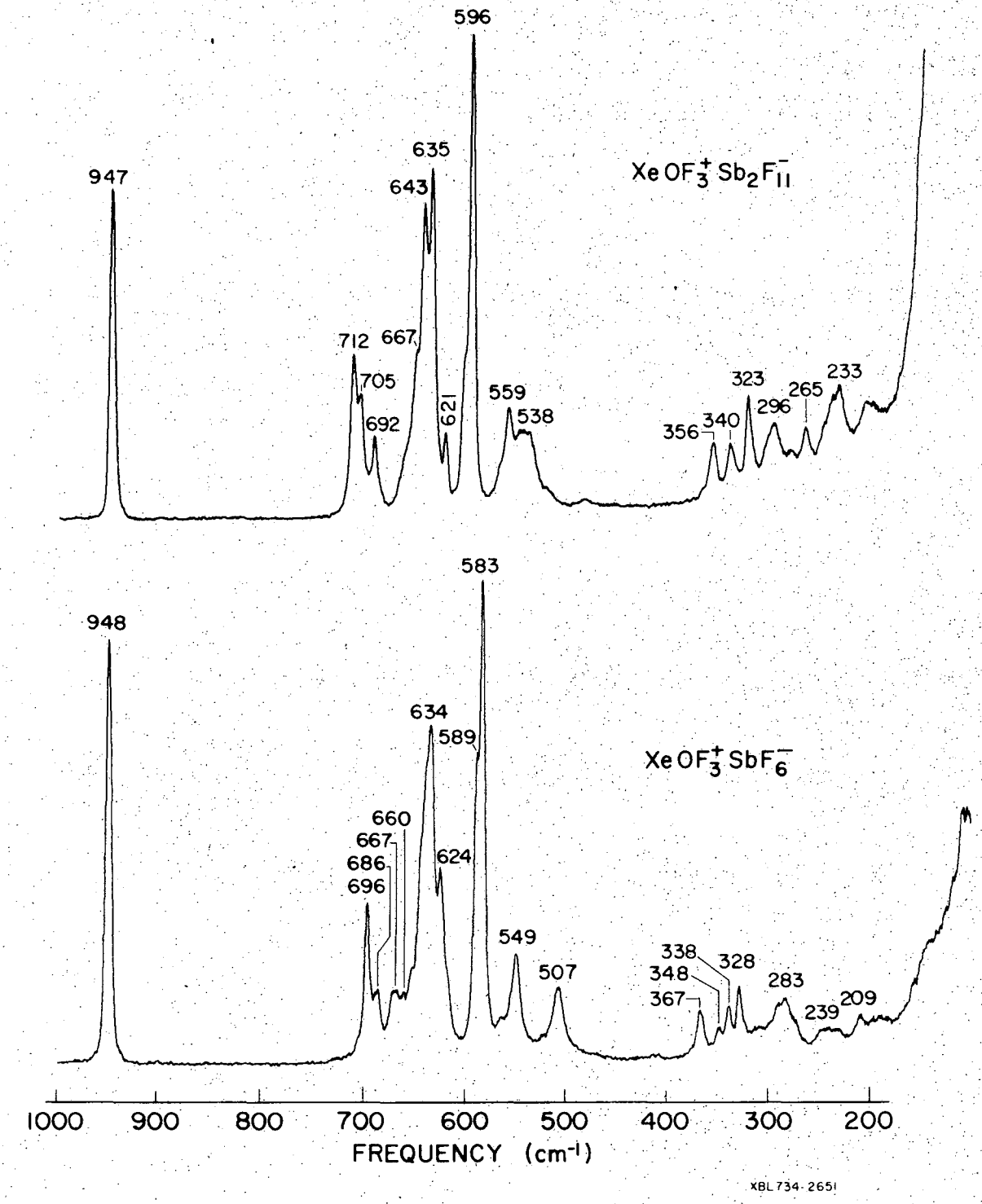


Figure III-1b Raman spectra of the $SbF_5$ salts of $XeOF_4$.

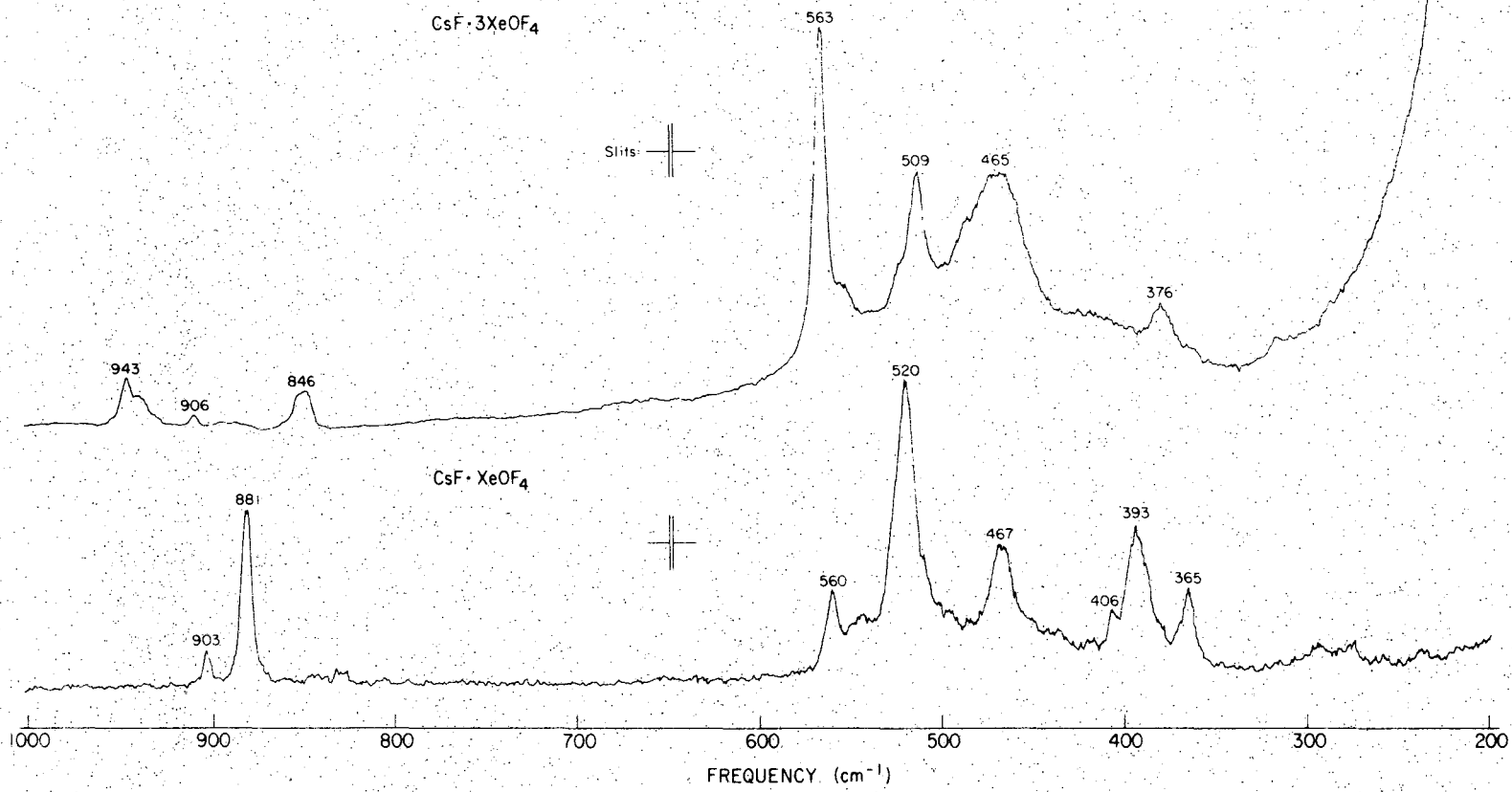


Figure III-2 Raman spectra of the CsF salts of $XeOF_4$.

XBL 723-6066

# IV. THE CRYSTAL STRUCTURE OF $XeF_3^+Sb_2F_{11}^-$

## A. Introduction

The 1:2 $XeF_4 \cdot SbF_5$ complex was made and investigated as described in the preceding chapter. The determination of its X-ray crystal structure was undertaken in order to complete the study. Of prime interest was confirmation of the proposed formulation $XeF_3^+Sb_2F_{11}^-$, and the determination of the geometry of the $XeF_3^+$ species. The influence of non-bonding electrons on cation geometry and coordination was a major concern.

## B. Experimental

Crystals of $XeF_3^+Sb_2F_{11}^-$ were grown by burying a Pyrex bulb containing a solution of $XeF_4$ in excess $SbF_5$, in a sand bath hot enough ( 50°) to accomplish complete solution. The temperature of the bath was reduced over a two day period to room temperature. The $SbF_5$ was distilled at room temperature from the yellow crystals under dynamic vacuum to traps held at -196°. Pumping was continued for several days to thoroughly dry the crystals. A Raman spectrum of a conglomerate of crystals showed that they were the 1:2 compound.

## C. Crystal Data

$XeF_4 \cdot 2SbF_5$ (mol. wt. 640.8) is triclinic with $\underline{a}$ = 8.237(5), $\underline{b}$ = 9.984(20), $\underline{c}$ = 8.004(5), $\underline{\alpha}$ = 72.54(5), $\underline{\beta}$ = 112.59(7), $\underline{\gamma}$ = 117.04(21)°,

$\underline{V}$ = 534.9 Å$^3$, $\underline{z}$ = 2, $\underline{d}_c$ = 3.98 g cm$^{-3}$, and F(000) = 559.86. Single crystal precession and Weissenberg photographs indicated that the space group is triclinic. A Delaunay reduction of the cell chosen failed to show additional symmetry. The structure was successfully refined in the space group $P\bar{1}$.

## D. X-Ray Measurements

A clear, roughly cubic crystal of edge 0.10 to 0.15 mm was chosen for data collection. A Picker automatic four circle diffractometer, equipped with a fine focus Mo anode tube, was used. High angle reflections were accurately centered at a take off angle of ~2° and were used for a least-squares refinement of the cell parameters. Data were collected and treated as described elsewhere.[41] A complete hemisphere of data was collected for $2\theta \leq 55°$. Intensities of three standards were collected at intervals of every 200 reflections. A total of 2662 intensity data were recorded.

## E. Structure Refinements

The least-squares program used in the structure refinements has been described.[42] Scattering factors for neutral fluorine, xenon, and antimony were used as given by Doyle and Turner.[43] Anamolous dispersion factors were given by Cromer and Liberman.[44]

Since the intensities of the standards were observed to diminish (finally to 85% of the original values) in a regular and nearly isotropic

manner, the data were scaled linearly between each pair of standards. Associated with this decrease was also noted a decrease in the parameters $\underline{b}$ and $\underline{\gamma}$ (which were in the end reduced by 0.2 Å and .21° from the initial values). Broadening of the omega scans of the standards from .10 to .35° was also observed. The positions of the heavy atoms were determined from a three dimensional Patterson synthesis. These positions were subjected to least-squares refinement as xenon atoms, after which it was possible to separate the antimony atoms by exploiting temperature factor differences. The positions were then further refined. A difference Fourier revealed positions for 12 of the 14 fluorine atoms. Least-squares refinement of these positions was followed by another difference Fourier which revealed the positions of the final two fluorine atoms. Refinement of all these positions, with anisotropic temperature factors, resulted in a conventional R factor of .06.

Examination of the observed and calculated structure factors showed that the poorest agreement occurred with the low angle, high intensity reflections. Since absorption and extinction corrections could not be reliably made, the lower angle data ($\sin \theta/\lambda \leq .32$) were given zero weight in the final least-squares refinements. This procedure resulted in R = 0.035, $R_2$ = .03, and a standard deviation for an observation of unit weight of 3.7. The number of non-zero weighted data in this refinement was 1823. The positional and thermal parameters, reported in Table IV-1, are from this refinement. Observed structure factors, standard deviations and differences are given in Table IV-2. The highest peak on a final difference Fourier proved to be only 2 e/Å$^3$. Table IV-3 gives chemically significant distances and angles.

## F. Description of Structure

The xenon atom is close-coordinated to three F atoms which define an approximately T-shaped species (Fig. IV-1a). The remaining atoms define an $Sb_2F_{11}$ unit which consists of two approximately octahedral $SbF_6$ groups, sharing a common F atom, such that the angle (Sb(1)-F-Sb(2)) is 155.4(2)°. The bridging Sb-F interatomic distances (average distance-2.02 Å) are significantly longer than the non-bridging, with the exception of that F atom (F(2)) which makes a close approach, of 2.50(1) Å, to the Xe atom. The interatomic Sb-F(2) distance is 1.90(1) Å. It is of interest that the F atom which makes this close approach to the Xe atom, is in cis relationship to the F atom of the Sb(1)-F-Sb(2) bridge.

The $Sb_2F_{11}$ species seen in this structure is similar to those previously reported,[13,15] but the $XeF_3$ species is novel. Only the bridging Sb-F distances differ significantly from 1.85 Å.

As Fig. IV-3 illustrates, all four atoms of the $XeF_3$ species are in the same plane, but, furthermore, the F(2) atom of the $Sb_2F_{11}$ unit, which makes the close approach of 2.50 Å to the Xe atom, is also in the same plane. Three other Xe contacts, to F(13), F(3) and F(7), of 2.94(1), 2.97(1), and 3.04(1), respectively, are made between formula units, as may be discerned from the stereogram given as Fig. IV-2, in conjunction with Fig. IV-1a.

## G. Discussion

The observed structure is consistent with the salt formulation of $XeF_3^+Sb_2F_{11}^-$. Other $Sb_2F_{11}$ salts reported[13,15] hitherto are $XeF^+Sb_2F_{11}^-$ and $BrF_4^+Sb_2F_{11}^-$. The $Sb_2F_{11}^-$ ion geometry has been discussed by Lind and Christe.[15]

Although the short in-plane contact of 2.50(1) Å between the $XeF_3^+$ ion and the closest F atom (F(2)) of an anion could be represented as an indication of some covalency, the ionic model provides a simple and direct accounting for the observed structural features, if due allowance is made for the polarizing character of the cation.

Regardless of which bonding model is used for the $XeF_3^+$ cation, one concludes that two non-bonding valence-electron pairs of the xenon atom are not involved in bonding. If the two non-bonding valence electron pairs are allowed to be sterically active then they will, with the three F-ligands, constitute a five coordinate arrangement for the xenon atom. As with the majority of five-coordinate non-transition element compounds, one might therefore expect the geometry to be based on a trigonal bipyramid.[46] Since the species $ClF_3$ and $BrF_3$ (which are electronically related to $XeF_3^+$) are T-shaped,[47,48] one could therefore anticipate that the $XeF_3^+$ non-bonding pairs would be in the equatorial plane as illustrated in Fig. IV-4. Such a cation would be far from spherical in its polarizing effect on anions. Indeed, the screening effects and repulsive effects of the non-bonding electron pairs and the F-ligands should result in a negatively charged species (such as a F-ligand of an anion) making an approach to the triangular faces containing the two non-bonding

electron pairs, as illustrated in Fig. IV-4. It is significant that the F(1)-Xe-F(2) angle of Fig. IV-3 is 154° and not 180°, and that all four F atoms close to the Xe atom are in the same plane.

It is instructive to compare $XeF_3^+$ with $XeF^+$ and $XeF_5^+$. In $XeF^+$ we have three non-bonding valence-electron pairs; therefore, the xenon coordination is pseudo-tetrahedral is illustrated in FIg. IV-4. This model indicates that a negatively charged species approaching $XeF^+$ would "see" the greatest positive charge when placed on axis trans to the F-ligand. This model accounts for the geometry of the $XeF^+Sb_2F_{11}^-$ arrangement reported by Peacock and his coworkers[13] and for the structure of $XeF^+RuF_6^-$ recently determined in these laboratories.[21] On the other hand, the $XeF_5^+$ ion possesses only one non-bonding xenon valence-electron pair and the xenon coordination is pseudo-octahedral. The crystal electron pair and the xenon coordination is pseudo-octahedral. The crystal structures of the $XeF_5^+$ salts[20,49-52] are in excellent accord with the maximum polarizating capability of this ion being directed in a cone about the symmetry axis as shown in Fig. IV-4.

Therefore, the $XeF_3$ species seen in the $XeF_3^+Sb_2F_{11}^-$ structure quite reasonably represents the geometry of the cation $XeF_3^+$. It is anticipated that the close similarity in shape observed for other isoelectronic species, e.g. $SF_3^+$ and $PF_3$ (ref. 42), and $XeF_5^+$ and $IF_5$ (ref. 21), will hold for $XeF_3^+$ and $IF_3$ and that the F(equatorial)-I-F(axial) angle will again be close to 80°.

As may be seen from Table IV-4 and Fig. IV-3, the axial bonds in $XeF_3^+$, $ClF_3$ and $BrF_3$ are significantly longer than the equatorial. All

bonds are shorter than in $XeF_4$, where Xe-F = 1.95 Å.[53] Evidently the equatorial F-ligand is more strongly bound than the axial ligands. This is in accord with the Pimentel and Rundle models,[54] in which the axial bonds are formulated as three center bonds (with the bonds amounting to single electron bonds) and the equatorial bond represented as an electron-pair bond. Alternatively, the greater length of the axial bonds can be attributed, on the basis of the electron pair repulsion model,[47] to the greater repulsive interaction of the axial F-ligands with the non-bonding electron pairs (which are at 90°); the equatorial ligand is at 120° from those electron pairs.

The length of the equatorial Xe-$F^+$ bond compares closely with that of Xe-$F^+$, as predicted[39] on the basis of the Xe-F bonds in $XeF_2$ being of bond order 0.5, and with that observed[13] in $XeF^+Sb_2F_{11}^-$. This is certainly consistent with an electron-pair representation. The axial Xe-F bonds are significantly shorter than Xe-F in $XeF_4$, but this shortening can be attributed to increase in the Xe-F bond polarity following the loss of $F^-$ and consequent increase in the effective positive charge of the xenon atom.

TABLE IV-1

Positional and Thermal Parameters for $XeF_3^+Sb_2F_{11}^-$
(Standard Deviations are in Parentheses)

| Atom | x | y | z | B11 | B22 | B33 | B12 | B13 | B23 |
|---|---|---|---|---|---|---|---|---|---|
| Xe | .29614(8) | .74522(6) | .18648(6) | 3.01(2) | 2.69(2) | 2.17(2) | 1.54(2) | 1.19(2) | .12(1) |
| Sb(1) | .12219(8) | .28979(6) | .50926(6) | 2.37(2) | 2.56(2) | 1.83(2) | 1.16(2) | .87(2) | - .37(1) |
| Sb(2) | .35701(8) | .22795(6) | .20527(7) | 2.75(2) | 2.71(2) | 1.91(2) | 1.16(2) | 1.09(2) | - .42(1) |
| F(1) | .1925(7) | .2154(6) | .3502(7) | 3.2(2) | 3.2(2) | 3.2(2) | 1.0(2) | 1.8(2) | - .6(2) |
| F(2) | .1869(9) | .4790(6) | .3518(7) | 4.7(3) | 3.6(2) | 3.2(2) | 2.4(2) | 1.8(2) | .4(2) |
| F(3) | .3785(8) | .3544(7) | .6376(8) | 3.2(2) | 4.3(3) | 3.8(2) | 1.6(2) | - .6(2) | -1.7(2) |
| F(4) | .318(1) | .0264(6) | .3119(8) | 5.7(3) | 3.1(2) | 4.3(3) | 2.5(2) | 2.6(2) | .7(2) |
| F(5) | .078(1) | .0993(6) | .6485(8) | 6.1(3) | 3.1(2) | 3.6(2) | 1.9(2) | 3.1(2) | .8(2) |
| F(6) | .134(1) | .1604(8) | .0228(8) | 5.3(3) | 6.1(3) | 2.9(2) | 2.3(3) | .2(2) | -2.1(2) |
| F(7) | .510(1) | .2383(8) | .0782(8) | 5.0(3) | 5.9(3) | 4.1(2) | 2.6(3) | 3.1(2) | - .3(2) |
| F(8) | .057(1) | .3681(8) | .6462(8) | 7.1(4) | 5.8(3) | 4.1(2) | 3.9(3) | 3.2(3) | - .3(2) |
| F(9) | .273(1) | .8988(7) | -.0048(7) | 5.5(3) | 3.6(2) | 2.5(2) | 1.8(2) | 1.3(2) | 1.0(2) |
| F(10) | .0531(9) | .6367(7) | .0420(8) | 3.4(2) | 4.6(3) | 3.4(2) | 1.8(2) | - .4(2) | -1.2(2) |
| F(11) | .5350(8) | .9022(6) | .2669(8) | 3.5(2) | 3.3(2) | 4.6(3) | 1.4(2) | 1.3(2) | - .2(2) |
| F(12) | -.1162(9) | .2269(9) | .3476(9) | 2.8(2) | 6.6(4) | 4.2(3) | 1.3(2) | .1(2) | -2.1(2) |
| F(13) | .5594(8) | .2897(7) | .4117(7) | 3.4(2) | 5.8(3) | 2.7(2) | 2.2(2) | .5(2) | -1.0(2) |
| F(14) | .3726(9) | .4274(5) | .1226(7) | 4.7(3) | 2.1(2) | 3.9(2) | 1.2(2) | 2.2(2) | .4(2) |

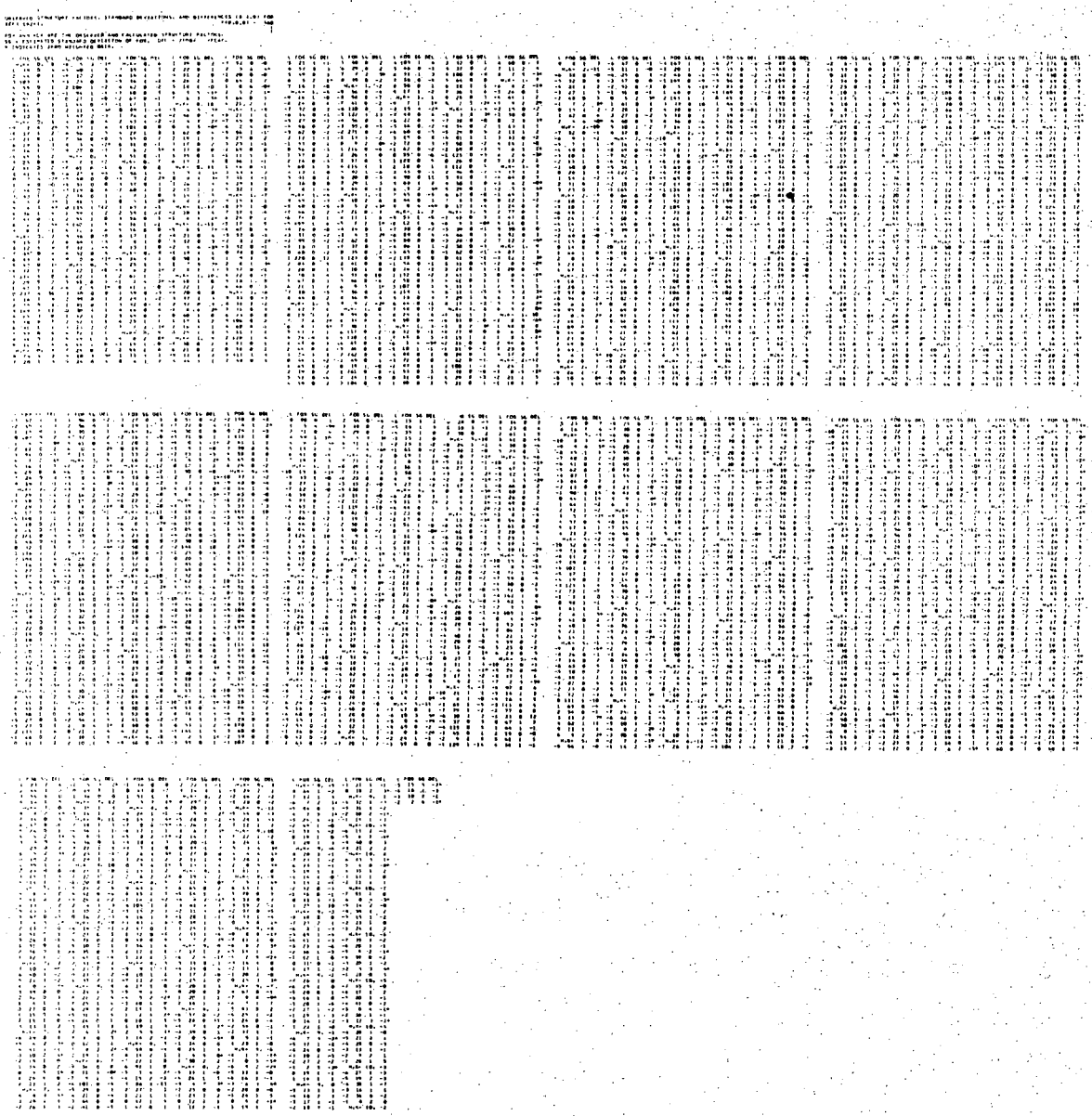

Table IV-2 Observed Structure Factors, Standard Deviations, and Differences (×1.0) for $XeF_3^+Sb_2F_{11}^-$

## Table IV-3

Interatomic Distances (Å) and Angles (Deg.) for $XeF_3^+Sb_2F_{11}^-$
(Standard Deviations 0.01 Å for all Distances)

| Intramolecular Distances | | Intramolecular Angles | | Intermolecular Distances (≤ 3.5 Å) | |
|---|---|---|---|---|---|
| Xe-F(2) | 2.50 | F(1)-Sb(2)-F(4) | 85.80(27) | Xe-F(3)[b] * | 2.97 |
| F(9) | 1.83 | F(6) | 86.30(30) | F(4)[j] | 3.17 |
| F(10) | 1.88 | F(7) | 178.81(37) | F(7)[c] | 3.04 |
| F(11) | 1.89 | F(13) | 85.07(25) | F(8)[e] | 3.26 |
| Sb(1)-F(1) | 2.01 | F(14) | 84.56(26) | F(13)[b] | 2.94 |
| F(2) | 1.90 | F(2)-Sb(1)-F(1) | 85.60(25) | F(1)-F(5)[f] | 2.91 |
| F(3) | 1.85 | F(3) | 86.26(32) | F(10)[e] | 3.34 |
| F(5) | 1.84 | F(5) | 171.94(37) | F(11)[b] | 3.28 |
| F(8) | 1.85 | F(8) | 91.24(31) | F(2)-F(3)[b] | 3.17 |
| F(12) | 1.83 | F(12) | 89.10(33) | F(8)[e] | 3.03 |
| Sb(2)-F(1) | 2.04 | F(3)-Sb(1)-F(1) | 85.24(29) | F(10)[e] | 3.24 |
| F(4) | 1.86 | F(5) | 90.78(34) | F(13)[b] | 2.91 |
| F(6) | 1.84 | F(8) | 95.29(35) | F(3)-F(3)[b] | 3.40 |
| F(7) | 1.85 | F(12) | 169.26(46) | F(7)[k] | 3.27 |
| F(13) | 1.86 | F(4)-Sb(2)-F(6) | 89.09(36) | F(11)[b] | 2.78 |
| F(14) | 1.86 | F(7) | 93.58(31) | F(13)[b] | 3.27 |
| F(1)-F(2) | 2.66 | F(13) | 88.91(32) | F(14)[b] | 2.84 |
| F(3) | 2.62 | F(14) | 170.35(38) | Xe[b] | 2.97 |
| F(4) | 2.66 | F(5)-Sb(1)-F(1) | 86.69(27) | F(4)-F(4)[d] | 3.45 |
| F(5) | 2.65 | F(8) | 96.50(32) | F(5)[f] | 3.02 |
| F(6) | 2.66 | F(12) | 92.52(37) | F(9)[ℓ] | 3.00 |
| F(13) | 2.64 | F(6)-Sb(2)-F(7) | 94.70(32) | F(11)[b] | 3.30 |
| F(14) | 2.63 | F(13) | 171.27(48) | F(11)[ℓ] | 2.77 |
| F(2)-F(3) | 2.56 | F(14) | 90.70(36) | F(12)[f] | 3.48 |
| F(8) | 2.68 | F(7)-Sb(2)-F(13) | 93.91(34) | F(5)-F(5)[f] | 3.06 |
| F(10) | 2.64 | F(14) | 96.05(32) | F(6)[k] | 3.06 |
| F(12) | 2.62 | F(8)-Sb(1)-F(1) | 176.76(36) | F(6)[f] | 3.47 |
| F(14) | 3.07 | F(12) | 94.49(39) | F(9)[m] | 3.23 |
| F(3)-F(5) | 2.63 | F(9)-Xe-F(10) | 81.73(30) | F(11)[b] | 3.00 |
| F(8) | 2.74 | F(11) | 80.22(30) | F(12)[f] | 3.40 |
| F(13) | 3.09 | F(2) | 154.39(38) | F(6)-F(6)[a] | 2.98 |
| F(4)-F(6) | 2.59 | F(10)-Xe-F(11) | 161.90(40) | F(8)[r] | 3.12 |
| F(7) | 2.71 | F(2) | 72.67(27) | F(9)[e] | 3.08 |
| F(13) | 2.61 | F(11)-Xe-F(2) | 125.34(31) | F(9)[ℓ] | 3.39 |
| F(5)-F(8) | 2.76 | F(12)-Sb(1)-F(1) | 84.76(29) | F(10)[e] | 2.89 |
| F(12) | 2.65 | F(13)-Sb(2)-F(14) | 89.84(33) | F(7)-F(9)[c] | 2.99 |
| F(6)-F(7) | 2.71 | Sb(1)-F(1)-Sb(2) | 155.37(15) | F(9)[ℓ] | 3.18 |
| F(14) | 2.63 | Xe-F(2)-Sb(1) | 171.64(13) | F(11)[ℓ] | 3.31 |
| F(7)-F(13) | 2.71 | | | F(11)[c] | 3.29 |
| F(14) | 2.76 | | | F(12)[n] | 3.04 |
| F(8)-F(13) | 2.70 | | | F(14)[c] | 3.12 |
| F(9)-F(10) | 2.43 | | | F(8)-F(8)[s] | 3.19 |
| F(11) | 2.40 | | | F(10)[s] | 2.95 |
| F(13)-F(14) | 2.63 | | | F(13)[b] | 3.50 |
| | | | | F(9)-F(9)[i] | 3.32 |
| | | | | F(11)[i] | 2.83 |
| | | | | F(12)[e] | 2.94 |
| | | | | F(10)-F(10)[e] | 2.67 |
| | | | | F(12)[e] | 3.15 |
| | | | | F(14)[e] | 3.06 |
| | | | | F(11)-F(12)[p] | 3.25 |
| | | | | F(13)[b] | 2.85 |
| | | | | F(12)-F(13)[q] | 3.25 |
| | | | | F(14)-F(14)[c] | 3.01 |

References for Table IV-3

* The crystal-chemical unit is at x,y,z and the letters refer to positions: a(-x,-y,-z); b(1-x,1-y,-z); c(1-x,1-y,-z); d(1-x,-y,1-z); e(-x,1-y,-z); f(-x,-y,1-z); g(-x,-1-y,-1-z); h(1-x,-y,-z); i(1-x,2-y,-z); j(x,1+y,z); k(x,y,1+z); ℓ(x,-1+y,z); m(x,-1+y,1+z); n(1+x,y,z); p(1+x,1+y,z); q(-1+x,y,z); r(x,y,-1+z); s(-x,1-y,1-z)

Table IV-4

Comparison of $ClF_3$, $BrF_3$ and $XeF_3^+$

| | $ClF_3$ | $BrF_3$ | $XeF_3^+$ |
|---|---|---|---|
| $E\text{-}F_{equatorial}$ (Å) | 1.598 | 1.721 | 1.83 |
| $E\text{-}F_{axial}$ (Å) | 1.698 | 1.810 | 1.88, 1.89 |
| $F_{ax}E\text{-}F_{eq}$ | 87.5° | 86.2° | 82°, 80° |
| Reference | 47 | 48 | this work |

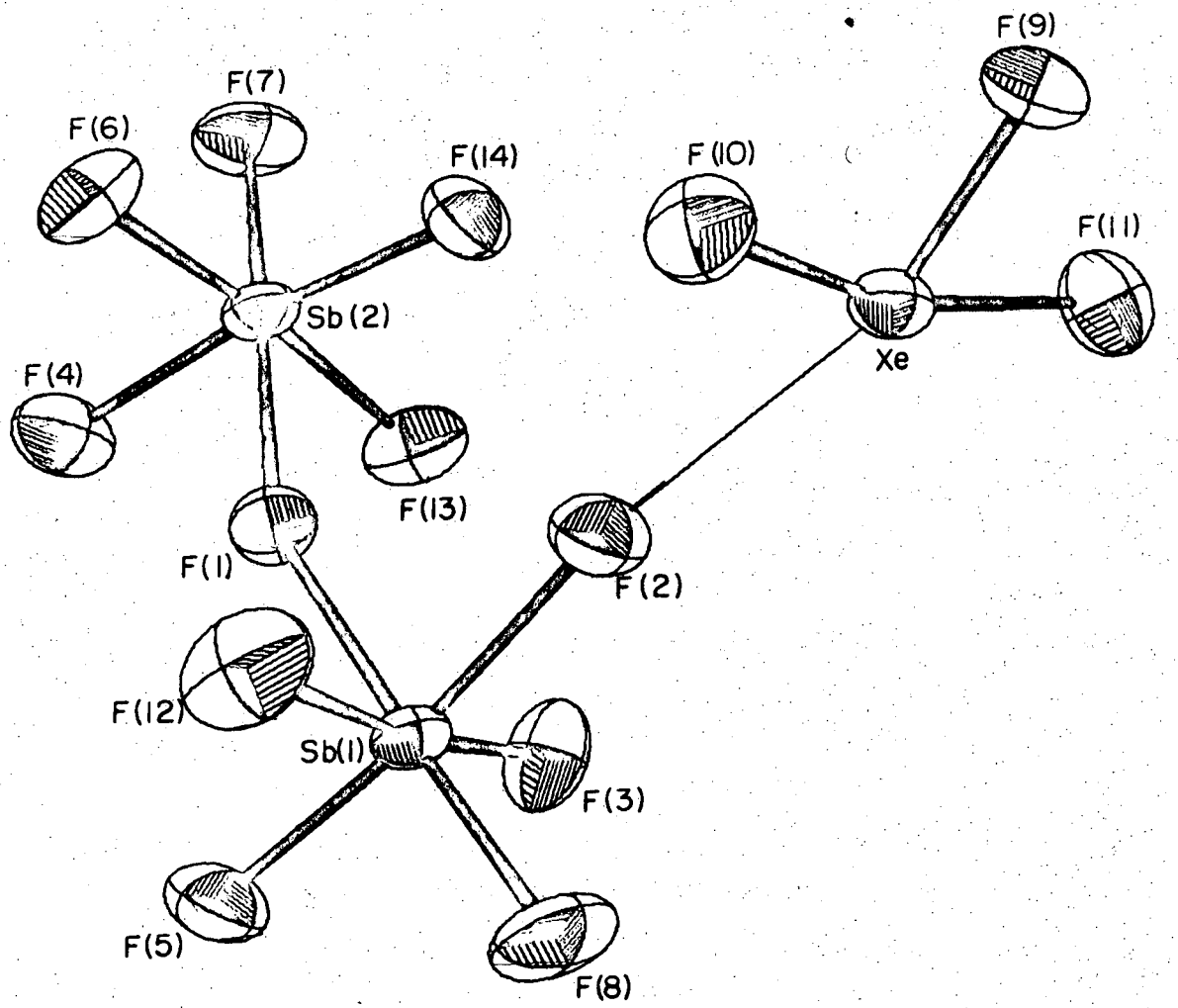


Figure IV-1a The structural unit $XeF_3^+Sb_2F_{11}^-$.

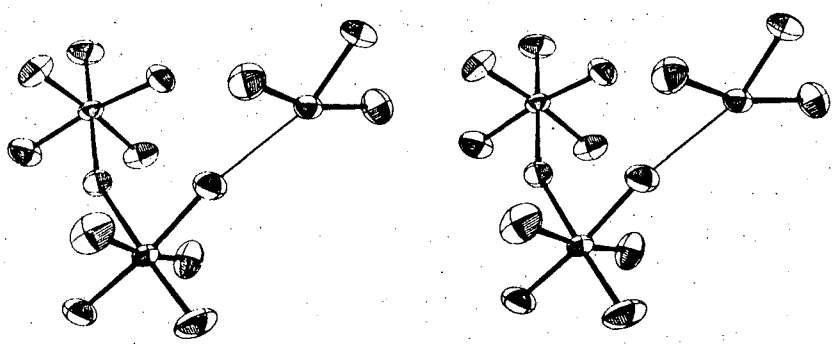

XBL 729-6974

Figure IV-1b Stereogram of the $XeF_3^+Sb_2F_{11}^-$ structural unit.

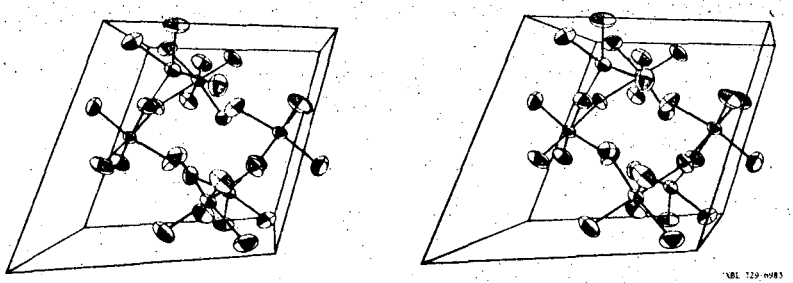

Figure IV-2 Stereogram showing the arrangement of the $XeF_3^+Sb_2F_{11}^-$ structural units within the unit cell; view along b.

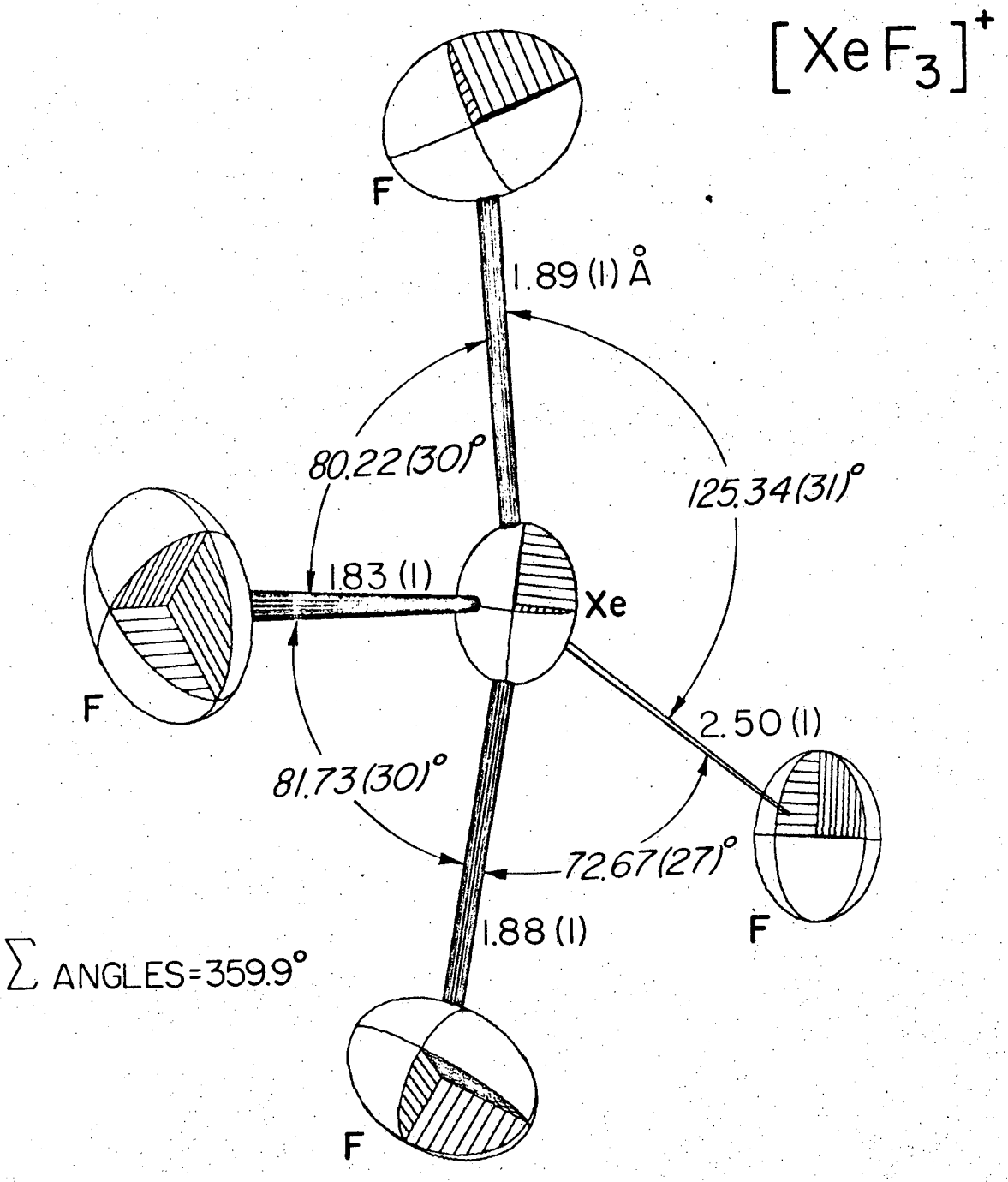


Figure IV-3 The $XeF_3^+$ ion and its close contact with the $Sb_2F_{11}^-$ ion.

XBL 729-6918

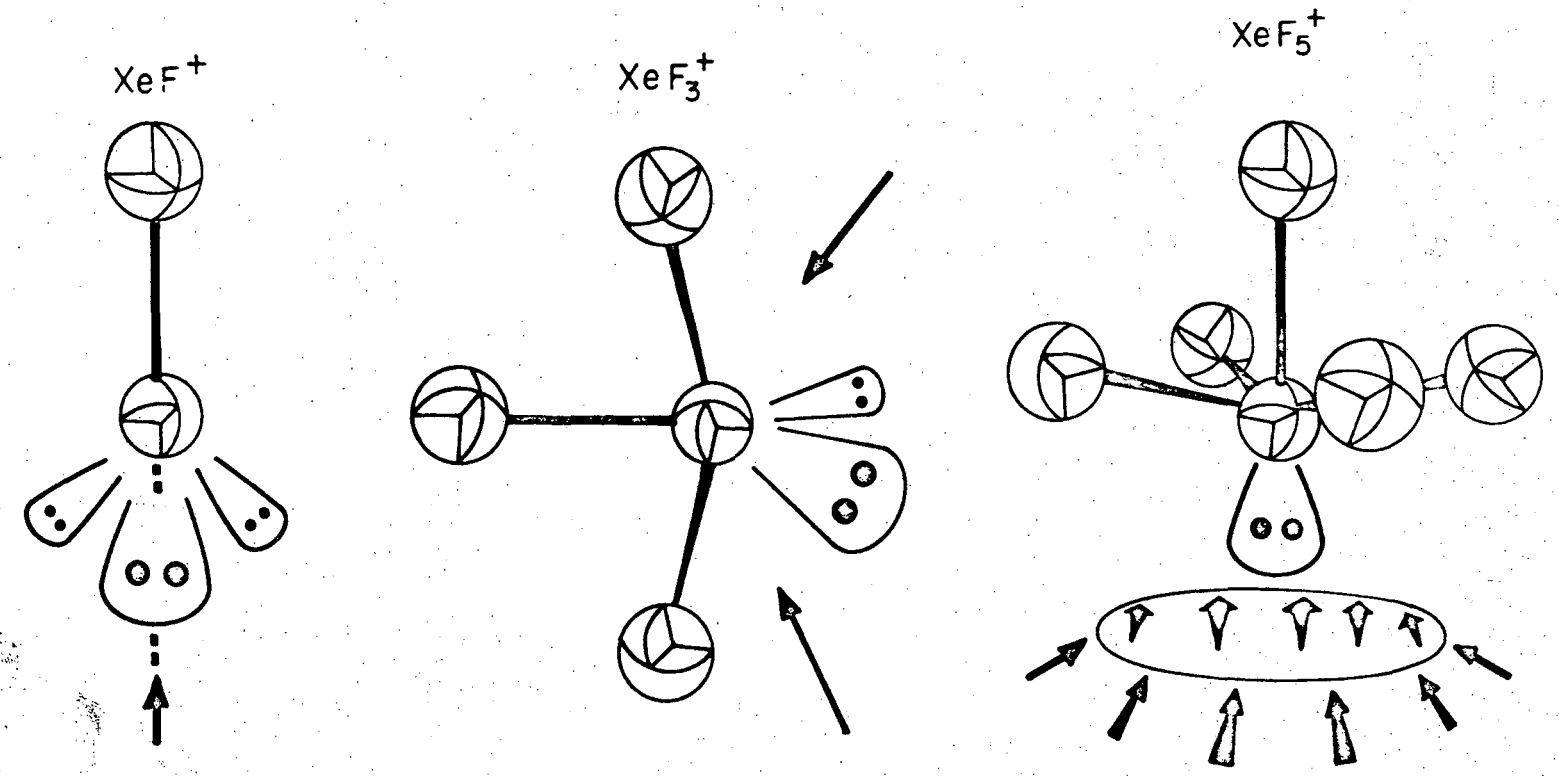


XBL728-6764A

Figure IV-4 Shapes of the $XeF_x^+$ ions based on steric activity of the non-bonding xenon valence electron pairs. (Arrows indicate directions of maximum polarizing effect.)

Footnote for Figure IV-4:

These models represent the non-bonding xenon electrons in a formalistic way. In the $Xe\text{-}F^+$ case the model cannot be realistic since such a cation has cylindrical symmetry. The postulated axial polarizing behavior can also be seen to be a consequence of Xe-F bond formation. Thus we can "synthesize" $(XeF)^+$ by bringing $F^+(^1D)$ up to the spherical Xe atom. If we use a p orbital pair of electrons of the Xe atom to form the Xe-F bond, the electron density will be diminished trans to the bond.

# V. IODINE, FLUORINE, XENON INTERACTIONS

## A. Introduction

As has been pointed out by Bartlett and Sladky,[55] the average bond energy of the xenon fluorides (which is approximately 30 kcal $mole^{-1}$ per bond) is less than for the average bond energy of any of the halogen fluorides. They also point out, however, that the addition of fluorine to the halogen monofluorides is comparable to the formation of noble gas fluorides. They particularly stressed the low thermodynamic stability of $IF_7$ relative to $IF_5$ and $F_2$. At the onset of this work, a questionable entity was the heat of formation of xenon difluoride. Several values had been reported,[56-58] measured by different techniques, and varying from -25.9 to -37 kcal $mole^{-1}$. The direct calorimetric value of -28.2 kcal $mole^{-1}$ for $\Delta H_f^o$ ($XeF_2$) seemed to be the most reliable.[56] Taken with the most dependable data for $IF_7$ and $IF_5$,[59] this suggested that $IF_7$ should be capable of oxidizing xenon to form xenon difluoride. The data presented in Table V-1 provide the basis for this prediction.

A study of the oxidation of $I_2$ by $XeF_2$ also seemed worthwhile, as rough bond energy estimates (Table V-2) showed that oxidations to $I^{I}$, $I^{III}$, and $I^{V}$ are definitely exothermic. Several experiments in acetonitrile solutions were carried out at low temperatures (-40°), in hopes of halting the oxidation at the +1 or +3 state and isolating the lower valence binary fluorides of iodine.

## B. Results and Discussion

The oxidation of xenon by $IF_7$ was accomplished at 280°, with the following reaction going to 84% completion:

$$Xe(g) + IF_7(g) \rightarrow XeF_2 \cdot IF_5(c) \quad . \qquad (1)$$

The crystalline product was found on the water-cooled lid of the reaction can.

The thermodynamic data (Table IV-1) show that reaction (2) is entropy driven, i.e., $\Delta H_{rxn}$ is essentially zero,

$$Xe(g) + IF_7(g) \rightarrow XeF_2(g) + IF_5(g) \qquad (2)$$

and the entropy difference makes $\Delta G_{rxn}$ favorable by 4.52 kcal mole$^{-1}$ at 300°K. Since the reaction

$$XeF_2(g) + IF_5(g) \rightarrow XeF_2 \cdot IF_5(c) \qquad (3)$$

occurs spontaneously,[60] it is probable that an exothermic value of at least -25 kcal mole$^{-1}$ should be allowed for $\Delta G$ of this reaction. In light of a $\Delta G_{rxn}$ which is favorable by nearly 30 kcal mole$^{-1}$, it is surprising that reaction (1) is only 84% complete. Recent, more accurate determinations of $\Delta H_f(XeF_2)$[61,62] have verified that the value used in our calculations cannot be wrong by more than 2 or 3 kcal mole$^{-1}$. In a subsequent experiment, $XeF_2 \cdot IF_5$ was heated under 1 atmosphere of

nitrogen pressure at 280° for 7 hours and then quenched to room temperature. $IF_7$ was absent. It seems likely then that the $IF_7$ and Xe interaction just described had not attained equilibrium. Thermodynamic calculations (Table V-3) for the reaction

$$ClF_5(g) + Xe(g) \rightarrow ClF_3(g) + XeF_2(g) \qquad (4)$$

indicate that $ClF_5$ should also oxidize xenon.

The results of the $I_2$ oxidations by $XeF_2$ in acetonitrile solution are not well defined. $IF_5$ was identified by infrared and $^{19}F$ n.m.r. spectroscopy to be a reaction product, but it was not determined if the $IF_5$ arose directly as an oxidation product, or from disproportionation of lower oxidation state fluorides. Although not definitive, certain experiments did indicate intermediate iodine fluorides.

## C. Experimental

### 1. Reagents

Xenon gas (Matheson Co., Inc., Rutherford, N.J.) was used without purification. Iodine heptafluoride was prepared by fluorination of iodine pentafluoride (Matheson) at 150° in a prefluorinated 0.2 ℓ nickel can. 20.3 g (92 mmole) $IF_5$ was heated with 8 gm (210 mmole) $F_2$ for 1 hr. Excess fluorine was removed at -196°. An infrared spectrum of the product at room temperature established that the only product was $IF_7$.

2. Oxidation of Xe with $IF_7$

Xe and $IF_7$ were measured out in a 100 ml can to equal pressures (see below) and condensed into a 200 ml bolted-lid nickel can. This can, which had a teflon sealing gasket, was equipped with a Monel-stemmed Whitey valve, and had been previously treated with $F_2$ and $IF_7$. The vessel, charged with its reactant gases, was placed in a resistance furnace and heated to 280° for 7 hrs., during which time the upper regions were cooled by flowing water. Unreacted gases were then separated physically. Xenon gas was removed at -110° and transferred to the original measuring can, where the pressure of gas was determined at 25°. The unreacted $IF_7$ was removed at room temperature and measured in the same can. Equimolar quantities (see below) of Xe and $IF_7$ remained, equal to 16% of the initial amounts. The can was opened in the dry box, revealing a colorless solid on the lid and upper walls. The melting point (98°) and X-ray powder pattern confirmed that it was $XeF_2 \cdot IF_5$.

Pressures (in mm Hg) in a 100 ml can

| | Xe | $IF_7$ | |
|---|---|---|---|
| Initial | 700 | 700 | (4.10 mmoles) |
| Final | 110 | 115 | |

Table V-1

| | $Xe(g)$ + | $IF_7(g)$ → | $XeF_2(g)$ + | $IF_5(g)$ |
|---|---|---|---|---|
| $\Delta H_f^o$ (kcal/mole) | | -229.7 | -28.6 | -200.87 |
| $S^o$ (gibbs/mole) | 40.529 | 83.08 | 62.05 | 79.96 |

$\Delta H_{rxn}$ = + 0.23 kcal/mole

$\Delta S_{rxn}$ = +17.41 gibbs/mole

$\Delta G_{rxn}^{300°K}$ = 0.23 - 4.75 = 4.52 kcal/mole

Thermodynamic values are from reference 59.

Table V-2

Bond Energy Differences*

| | | | | | | | | | Total |
|---|---|---|---|---|---|---|---|---|---|
| $I_2$ | + | $XeF_2$ | → | 2IF | + | Xe | | | |
| 45 | | 64 | | 2(67) | | | | | -25 |
| IF | + | $XeF_2$ | → | $IF_3$ | + | Xe | | | |
| 67 | | 64 | | 195 | | | | | -54 |
| $IF_3$ | + | $XeF_2$ | → | $IF_5$ | + | Xe | | | |
| 195 | | 64 | | 315 | | | | | -56 |
| $IF_5$ | + | $XeF_2$ | → | $IF_7$ | + | Xe | | | |
| 315 | | 64 | | 385 | | | | | - 6 |

* Estimates based on mean thermochemical bond energies:

| | M.T.B.E. | Ref. |
|---|---|---|
| $XeF_2$ | 32 | 56 |
| IF | 67 | 59 |
| $IF_3$ | 65 | interpolated |
| $IF_5$ | 63 | 59 |
| $IF_7$ | 55 | 59 |

Table V-3

| | $Xe(g)$ + | $ClF_5(g)$ → | $XeF_2(g)$ + | $ClF_3(g)$ |
|---|---|---|---|---|
| $\Delta H_f^o$ (kcal/mole) | | -54.9 | -28.6 | -37.97 |
| $S^o$ (gibbs/mole) | 40.529 | 74.241 | 62.05 | 67.279 |

$\Delta H_{rxn}$ = - 11.57 kcal/mole

$\Delta S_{rxn}$ = + 14.559 gibbs/mole

$\Delta G_{rxn}^{300°K}$ = -11.57 - 4.37 = - 15.94 kcal/mole

Thermodynamic values are from reference 59.

# VI. STUDIES OF KRYPTON (II) CHEMISTRY

## A. Introduction

Only two compounds of krypton are known: $KrF_2$ and $KrF_2 \cdot 2SbF_5$. The difluoride is thermodynamically unstable[63-65] and decomposes above -60°. However, the adduct with antimony pentafluoride was reported by its discoverers[66] to have greater stability, melting with decomposition at 50°. The salt formulation $KrF^+Sb_2F_{11}^-$ seemed possible for this compound, in light of the crystal structure[14] of its xenon analogue, $XeF_2 \cdot 2SbF_5$, which supported the formulation $XeF^+Sb_2F_{11}^-$. If that were the case, $KrF_2 \cdot 2SbF_5$ promised to have extraordinary oxidizing capability (see Section VI-D). The purpose of this study, then, was to prepare gram amounts of the krypton difluoride, antimony pentafluoride complex, determine its structure, if possible, and exploit its oxidizing potential in chemical reactions.

## B. Preparation of $KrF_2$

The thermodynamic instability of $KrF_2$ renders its synthesis difficult. The initial preparations for this study were by low temperature electric discharge of krypton and fluorine, according to the procedure described by V$_{on}$ Grosse, *et al.*,[65] the essential apparatus for which is shown in Fig. VI-1. Extensive use of a nearly identical apparatus yielded small amounts of $KrF_2$. Several modifications of the original technique were made in an effort to increase the efficiency and lower

the cost of the operation. Attack by the fluorine on the electrodes and on the Pyrex cell itself was severe. A discharge cell with replaceable copper electrodes was the greatest improvement, permitting many hours of operation before etching of the Pyrex necessitated the building of a new unit. To make them replaceable, the electrodes were sealed through Swagelock fittings provided with Teflon ferrules, rather than solder connections as in the original apparatus.

As shown in Fig. VI-2, a knife-edge and indium metal ring were employed to seal the electrode support to the Pyrex cell. A series arrangement of two such horizontal discharge tubes received the most use, the electrodes being replaced every few days as necessitated by instability of the electric arc on the corroded surfaces. A variety of electrode tip shapes were tried, including cones, hemispheres, and flat surfaces; the flat surfaces seemed to be best. Nickel plated electrodes were more quickly rendered inoperable than unplated copper ones. The final modification (Fig. VI-3), prompted by the observation by Falconer[67] that vertical discharges yielded more $KrF_2$ than horizontal ones, was the easiest to disassemble for electrode exchange, but was not used enough to allow a quantitative comparison to the horizontal arrangement.

Regardless of all the efforts to improve and cheapen the manufacture of the system, the electric discharge technique remained inefficient, and unsuitable for producing large enough quantities of $KrF_2$ (of the order of 0.5-1.0 gm) for macroscopic chemical reactions. The proton bombardment technique of Mackenzie[68] was, therefore, employed.

The apparatus for proton bombardment is shown in Fig. VI-4. The 2 liter aluminum can was filled to a pressure of 2 atmospheres with a 1:1 mixture of fluorine and krypton, and exposed to a 10 MeV stream of protons from the 88-inch cyclotron. A high liquid nitrogen level about the copper straps was maintained throughout the 1-6 hr. bombardments by an automatic filling device. This kept the temperature of the reaction can at -130°. A television monitor inside the cyclotron cave allowed the pressure to be observed during the bombardments. As the gaseous reactants formed solid $KrF_2$, which froze to the sides of the can, the pressure steadily dropped. After the termination of the bombardment, the can was returned to the vacuum system where unreacted gases were removed under vacuum. Only then was the liquid nitrogen removed from the cooling straps, and as the can began to warm slowly, the products were removed under dynamic vacuum and collected at -196° in a storage trap. The sublimation of solid $KrF_2$ began at ca. -50°. Pumping was continued until the can reached room temperature, a matter of 30-45 minutes, a time sufficient to insure collection of all the product. HF and any other volatile impurities were removed under vacuum at -78°, the temperature at which the $KrF_2$ was stored. Yields from this preparation were never as high as the reported one gram per hour of irradiation,[68] but of the order of one-fourth to one-half of that. Cost was the restricting factor of this technique, being $150 per hour of cyclotron time. This synthesis provided material for the reactions described below.

## C. Preparation and Characterization of $KrF_2 \cdot 2SbF_5$

The 1:2 adduct of $KrF_2$ and $SbF_5$ was most often prepared in the Kel-F or quartz trap in which the $KrF_2$ was stored, minimizing decomposition of the $KrF_2$ which occurs while transferring it. Quartz is preferred over Kel-F, as the krypton-containing compound cracked Kel-F containers on occasion. The preparation of $KrF_2 \cdot 2SbF_5$ required particularly dry $SbF_5$. After repeated vacuum distillations, as a final purification the $SbF_5$ was distilled onto $XeF_2$ at -196°, then warmed to room temperature. The $SbF_5$ in excess over the $XeF_2 \cdot 2SbF_5$ which formed was then distilled onto the $KrF_2$. The bottom of the reaction vessel, containing the $KrF_2$, was held at -196° while the $SbF_5$ at the top melted and was allowed to run down onto the $KrF_2$. The liquid nitrogen was then removed, and as the vessel slowly warmed, a reaction was seen to occur, as evidenced by bubbling and formation of a white mist above the solution. The excess $SbF_5$ was removed at room temperature under the best dynamic vacuum available, as the complex in $SbF_5$ solution is less stable than when isolated and free of solvent. The white solid which remained was subjected to an additional hour of pumping (after it was apparently free of $SbF_5$) to insure complete removal of the solvent.

The formulation of the complex so prepared as $KrF^+Sb_2F_{11}^-$ is based on the Raman spectrum (Fig. VI-5) and X-ray powder pattern (Fig. VI-6). The remarkable similarity to $XeF^+Sb_2F_{11}^-$ strongly suggests that the compounds are isostructural. The Raman spectrum was excited by the He-Ne 6328 Å line at 100 mw, and shows the Kr-F stretch at 626 $cm^{-1}$ (c.f., Xe-F in $XeF^+Sb_2F_{11}^-$ at 620 $cm^{-1}$), a value in close agreement with

620 $cm^{-1}$, the value calculated by Schaefer[69] for the $KrF^+$ ion. It has not been possible to index the powder pattern on the basis of the monoclinic cell found for $XeF^+Sb_2F_{11}^-$, but the similarity (Fig. VI-6) indicates that only slight parameter shifts distinguish this pattern from that of the xenon compound.

## D. Energy Considerations

The $KrF^+$ ion promised to have considerable oxidizing capability, as illustrated by the thermodynamic cycle below (values in kcal $mole^{-1}$). The electron affinity of $KrF^+$ is seen to be the ionization potential of krypton, less the difference in bond energy between $KrF^+$ and KrF. This difference is not expected to be greater than 40 kcal, so the electron affinity of $KrF^+$ is, therefore, at least 280 kcal/mole. Furthermore, a species oxidized by the action of $KrF^+$ in the salt $KrF^+Sb_2F_{11}^-$ is likely to be stabilized by the very strong anion $Sb_2F_{11}^-$, making this salt additionally attractive as an oxidizer.

$$
\begin{array}{ccc}
KrF & \longleftarrow & KrF^+ + e \\
\Big\downarrow & & \Big\uparrow \\
Kr + F & \longrightarrow & Kr^+ + F + e
\end{array}
$$

B.E. (KrF) $\leq$ 12 (ref. 64)

B.E. ($KrF^+$) $\approx$ 38 (ref. 70)

I (Kr) = 323

## E. Reaction of $IF_5$ with $KrF^+Sb_2F_{11}^-$

The oxidation of $IF_5$ to $IF_7$ is one which is easily accomplished by fluorine itself, under moderate conditions of temperature and pressure. $IF_6^+$ salts are well-known and are readily identifiable by Raman spectroscopy.[71,72] Therefore it seemed instructive to investigate the interaction of $IF_5$ with $KrF^+Sb_2F_{11}^-$, as a simple verification of the energy considerations and a preliminary experimental probe into the techniques which such systems would require. Equation (1) was the anticipated result:

$$IF_5 + KrF^+Sb_2F_{11}^- \rightarrow IF_6^+Sb_2F_{11}^- + Kr \qquad (1)$$

The reaction was carried out in a Kel-F trap, in which a few hundred milligrams of the salt had been placed. Sufficient $IF_5$ (2-3 ml), established to be free of $IF_7$, was distilled into the trap to serve as a solvent as well as a reactant. Interaction of the two compounds was seen to occur at approximately -20°, as the liquid $IF_5$, running down the sides of the trap, came into contact with the solid $KrF^+Sb_2F_{11}^-$. As interaction occurred, krypton gas evolved and the solid changed in appearance. When gas evolution had ceased the excess $IF_5$ was removed under dynamic vacuum at room temperature, and a Raman spectrum of the remaining solid established the presence of the $IF_6^+$ species. Raman characterizations of the salts $IF_6^+SbF_6^-$ and $IF_6^+Sb_2F_{11}^-$ have still not been reported and were not made in this study. We are therefore unable

to identify the product unambiguously but we are sure that the cation species is $IF_6^+$. This was sufficient for the purpose of the experiment.

## F. Reaction of $BrF_5$ with $KrF^+Sb_2F_{11}^-$

It seemed possible that $KrF^+$ (in the $Sb_2F_{11}^-$ salt) could oxidize $BrF_5$ to form the new species $BrF_6^+$. The reaction was carried out in a manner identical to the $IF_5$ reaction. The $KrF^+Sb_2F_{11}^-$ dissolved in the $BrF_5$, accompanied by bubbling of the mixture and a clear solution was eventually obtained. When the $BrF_5$ was removed under vacuum at room temperature, a white solid remained, which was identified by comparison of its Raman spectrum with that from an authentic sample, as $BrF_4^+Sb_2F_{11}^-$ (ref. 13). The acid-base reaction

$$BrF_5 + KrF^+Sb_2F_{11}^- \rightarrow KrF_2 + BrF_4^+Sb_2F_{11}^- \qquad (2)$$

took preference over the oxidation-reduction reaction, and presumably the displaced $KrF_2$ decomposed upon warming.

## G. Reaction of $ClF_5$ with $KrF^+Sb_2F_{11}^-$ and Related Reactions

$ClF_6^+$ (in the $PtF_6^-$ salt) has been prepared by Christe, *et al.*,[73] through the use of ultraviolet excitation. Their products are not pure, however, and the oxidation of $ClF_5$ with $KrF^+Sb_2F_{11}^-$ to give a pure product, $ClF_6^+Sb_2F_{11}^-$ seemed hopeful.

The reaction was carried out similarly to the $IF_5$ and $BrF_5$ reactions, using quartz and sapphire reaction vessels. Reactions of $KrF_2$, $ClF_5$ and

either $PtF_6$ or $SbF_5$ were also tried, in which nearly stoichiometric amounts of the three reactants were distilled into the reaction vessel and warmed to room temperature together. These experiments are tabulated below (Table VI-1). In no case were the Raman bands assigned by Christe[73] to $ClF_6^+$ seen in the solid products. Attack on the reaction vessels, both quartz and sapphire, was sufficient to give oxygen containing products; e.g., $ClO_2^+$. The presence of $ClF_4^+$ in the reaction products was indicated by Raman spectroscopy. The $ClF_2^+$ species was also an identified product. These observations are in harmony with Passmore's[74] failure to prepare $ClF_6^+$ and $ClF_4^+$ from the interaction of $ClF_5$ with $IrF_6$. The only identified solid product from the latter reaction was determined to be $ClF_2^+IrF_6^-$. The reaction of $ClF_5$ with $KrF^+Sb_2F_{11}^-$ seems to be similar to that of $BrF_5$ in that a displacement reaction occurs:

$$ClF_5 + KrF^+Sb_2F_{11}^- \rightarrow KrF_2 + ClF_4^+Sb_2F_{11}^- \qquad (3)$$

Table VI-1

| | reaction vessel | identified products | comments |
|---|---|---|---|
| 1. $ClF_5 + KrF^+Sb_2F_{11}^-$ | quartz | $ClO_2^+$ | dark blue intermediate |
| 2. $ClF_5 + KrF^+Sb_2F_{11}^-$ | sapphire | $ClO_2^+$<br>$ClF_2^+$ | product decomposed at room temperature |
| 3. $KrF_2 + ClF_5 + SbF_5$ | quartz | $ClF_4^+$<br>$ClF_2^+$ | |
| 4. $KrF_2 + ClF_5 + PtF_6$ | quartz | none | possible leak in apparatus |

## H. Reaction of $XeOF_4$ with $KrF^+Sb_2F_{11}^-$ and Related Reactions

The $XeOF_4$ molecule was chosen as a likely species for oxidation by $KrF^+Sb_2F_{11}^-$. As with the halogen pentafluorides, its pseudo-octahedral geometry leaves a non-bonding pair of electrons exposed, and its isoelectronic relationship to $IF_5$ was encouraging, in light of the oxidation of that compound. The oxidation of $XeOF_4$ to $XeOF_5^+$ might provide a pathway to a stable $Xe^{VIII}$ oxyfluoride, $XeOF_6$.

The experiments were carried out in the same manner as with $IF_5$ and are tabulated below (Table VI-2). A small amount (~0.20 gm) of $KrF^+Sb_2F_{11}^-$ was placed in a Kel-F or quartz trap. $XeOF_4$ was distilled into the trap at -196°, then warmed and allowed to run down the sides of the trap onto the $KrF^+Sb_2F_{11}^-$. Upon contact of the reactants, at ca. -10°, a yellow color appeared, coinciding with bubbling and agitation of the reactants. The reaction proceeded differently from this point is the two instances it was carried out, as indicated in Table VI-2. In reaction 1, only enough $XeOF_4$ was used to cover the $KrF^+Sb_2F_{11}^-$, i.e., only an approximately stoichiometric amount of $XeOF_4$ was present, not enough to dissolve the krypton salt. The product of this reaction, "A", was a yellow solid. The Raman evidence on "A" indicated that it was a mixture of $XeOF_3^+SbF_6^-$, $KrF^+SbF_6^-$, and $O_2^+SbF_6$. This mixture was redissolved in anhydrous HF in a Kel-F tube to form a clear, yellow solution. The HF was removed under dynamic vacuum at 0° and a yellow solid remained. In experiment 2, sufficient $XeOF_4$ (2-3 ml) was used to serve as a solvent. The $KrF^+Sb_2F_{11}^-$ dissolved in it to form a clear,

Table VI-2

| | | |
|---|---|---|
| 1. | $XeOF_4 + KrF^+Sb_2F_{11}^- \rightarrow$ mixture "A" (see text) | approximately stoichiometric $XeOF_4$ |
| | "A", recrystallized from HF* $\rightarrow$ $XeOF_5^+Sb_2F_{11}^-$ | |
| 2. | $XeOF_4 + KrF^+Sb_2F_{11}^- \rightarrow$ $XeOF_5^+Sb_2F_{11}^-$ | excess $XeOF_4$ as solvent |
| 3. | $KrF_2 + AsF_5 + XeOF_4 \rightarrow$ $XeF_5^+AsF_6^-$ | approximately stoichiometric quantities condensed into a quartz trap; yellow solution, but a colorless product |
| 4. | $SbF_5 + XeOF_4 + KrF_2 \rightarrow$ $XeOF_3^+SbF_6^-$ | approximately stoichiometric quantities condensed into a quartz trap in the order indicated |

* Care had been taken to remove water from this HF by fluorinating the material supplied by Matheson with gaseous $F_2$.

yellow solution which left a yellow solid upon removal of the excess $XeOF_4$ under vacuum. This product and the final product of reaction 1 gave identical X-ray powder patterns (Table VI-5) and Raman spectra (Fig. VI-7). On the basis of subsequent studies (see below), mixture "A" was identified as $XeOF_5^+Sb_2F_{11}^-$. Reactions 3 and 4, involving $KrF_2$ rather than $KrF^+$ as the potential oxidizer, yielded the $Xe^{VI}$ compounds indicated, with no oxidation occurring.

Figure VI-7 compares the Raman spectrum of $XeOF_5^+$ in $XeOF_5^+Sb_2F_{11}^-$ with that of its isoelectronic relative $IOF_5$. The dotted lines connect bands of the cation to their related $IOF_5$ bands; the other bands in the $XeOF_5^+Sb_2F_{11}^-$ spectrum are assigned to the anion. Bands due to $O_2^+SbF_6^-$ and $O_2^+Sb_2F_{11}^-$, impurities arising from oxidation of the quartz reaction vessel, have been deleted. In $XeF_5^+$ certain of the $\nu$(Xe-F) bands are at lower frequency than in $IF_5$.[75] This effect is also seen for the $XeOF_5^+$, $IOF_5$ pair. Ligand crowding of the highly charged xenon (VI) and (VIII) species may account for these stretching frequency anamolies. The remarkable stability of $XeOF_5^+Sb_2F_{11}^-$ (m.p. = 70°, no decomposition) is in accord with the predicted pseudo-octahedral geometry of $XeOF_5^+$ and the previously noted stability apparently associated with species of such geometry.

Table VI-3

Raman Spectrum of $XeOF_5^+Sb_2F_{11}^-$

| | | |
|---|---|---|
| 918 (10) | $\nu$(Xe-O) | |
| 686 (40) | | $\nu$(Sb-F) |
| 665 (40) | | $\nu$(Sb-F) |
| 615 (100) | $\nu$(Xe-F) | |
| 572 (40) | $\nu$(Xe-F) | |
| 538 (30) | | $\nu$(Sb-F) |
| 515 (5) | | $\nu$(Sb-F) |
| 405 (5) | $\delta$(Xe-F) | |
| 368 (10) | $\delta$(Xe-F) | |
| 310 (4) | | $\delta$(Sb-F) |
| 290 (15) | | $\delta$(Sb-F) |

In an attempt to prepare $XeOF_6$, CsF and $XeOF_5^+Sb_2F_{11}^-$ were heated together in a quartz tube to 75°. No reaction or volatile products were observed. The presence in the remaining solid of a species containing xenon-oxygen bonds was indicated by its Raman spectrum. This implies that the $XeOF_7^-$ may be a very stable anion.

## I. Projections

The $KrF^+Sb_2F_{11}^-$ has proven itself as an extraordinary oxidizer. Indeed, under the proper conditions the $KrF^+$ species may be capable of oxidizing $BrF_5$ and $ClF_5$, as well as other untried compounds. $KrF^+PtF_6^-$ should be prepared from $KrF_2$ and $PtF_5$. Since $PtF_5$ is a weaker Lewis acid than $SbF_5$, one might avoid the acid-base displacement reactions that occurred in this study.

$XeOF_5^+Sb_2F_{11}^-$ should be prepared again and more fully characterized. A $^{19}F$ m.n.r. spectrum in $SbF_5$ solution would demonstrate the $C_{4v}$ symmetry of the cation, and an X-ray crystal structure determination would provide valuable bonding information.

Further attempts to displace $XeOF_6$ in a suitable solvent would be of great interest.

Figure VI-1. Diagram of original apparatus used for the preparation of krypton difluoride by the electric discharge method.

A: Polychlorotrifluoroethylene container for the collection and stroage of the compound, attached to the glass apparatus by compression fittings.

B and C: U-tubes of Pyrex glass with break seals.

D: Electrical discharge reaction vessel made of Pyrex glass (dia., 60 mm); height of wide portion, 200 mm). Two copper disks of 20 mm. diameter and 5 mm thickness, spaced 75 mm apart, serve as electrodes. The leads to the electrodes are silver soldered into Kovar to glass seals.

E: Valve manifold to convert push-pull operation of magnetic piston pump into unidirectional gas circulation as indicated. Each individual valve consisted of a 10-mm glass tube ground flat at the end, protruding into a wider tube and closed with a thin square piece of glass held in place by gravity. Application of a small pressure head from below (0.1 mm) permits gas to flow upward. Downward flow is inhibited by the closure of the ground end of the glass tube by the square piece of glass. Arrangement of four valves in the way indicated in the figure permits use of the pumping action of each half stroke of the piston.

F: Magnetic piston pump after Brenschede.[(a)]

G: Piston of pump suspended from stainless steel spring.

H: Solenoid.

V1, V2, V3: Monel valves. WIth the reaction in progress valve 1 is kept closed while valves 2 and 3 are open. During the purification and sublimation of the product, first to tube C and then into tube B, valves 2 and 3 are closed to separate the pump from the rest of the system, and valve 1 is open to establish a connection to the vacuum line.

(a) W. Brenschede, Z. Physik. Chem. (Leipzig) A178, 74 (1936-37).

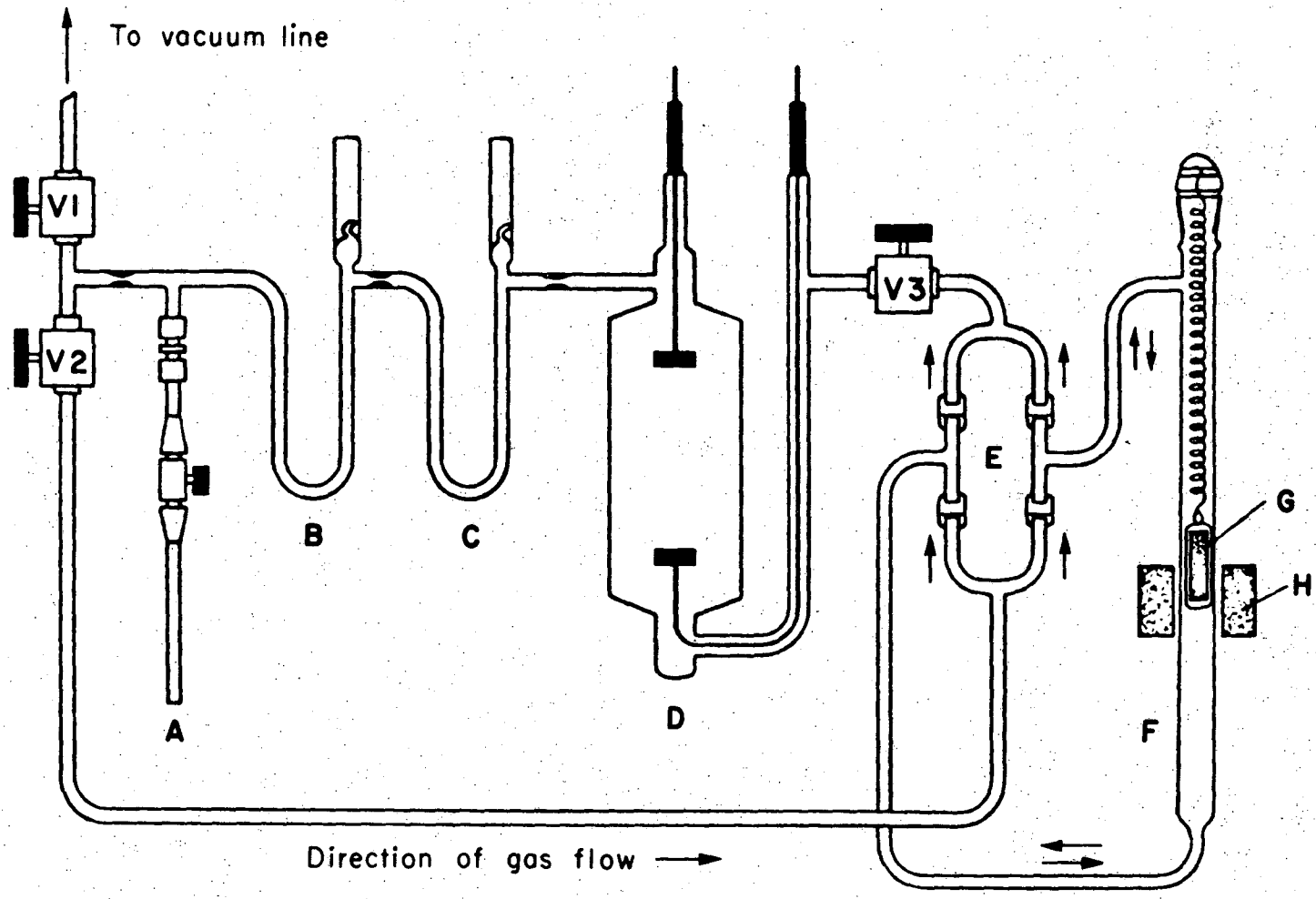


Figure VI-1

XBL704-2667

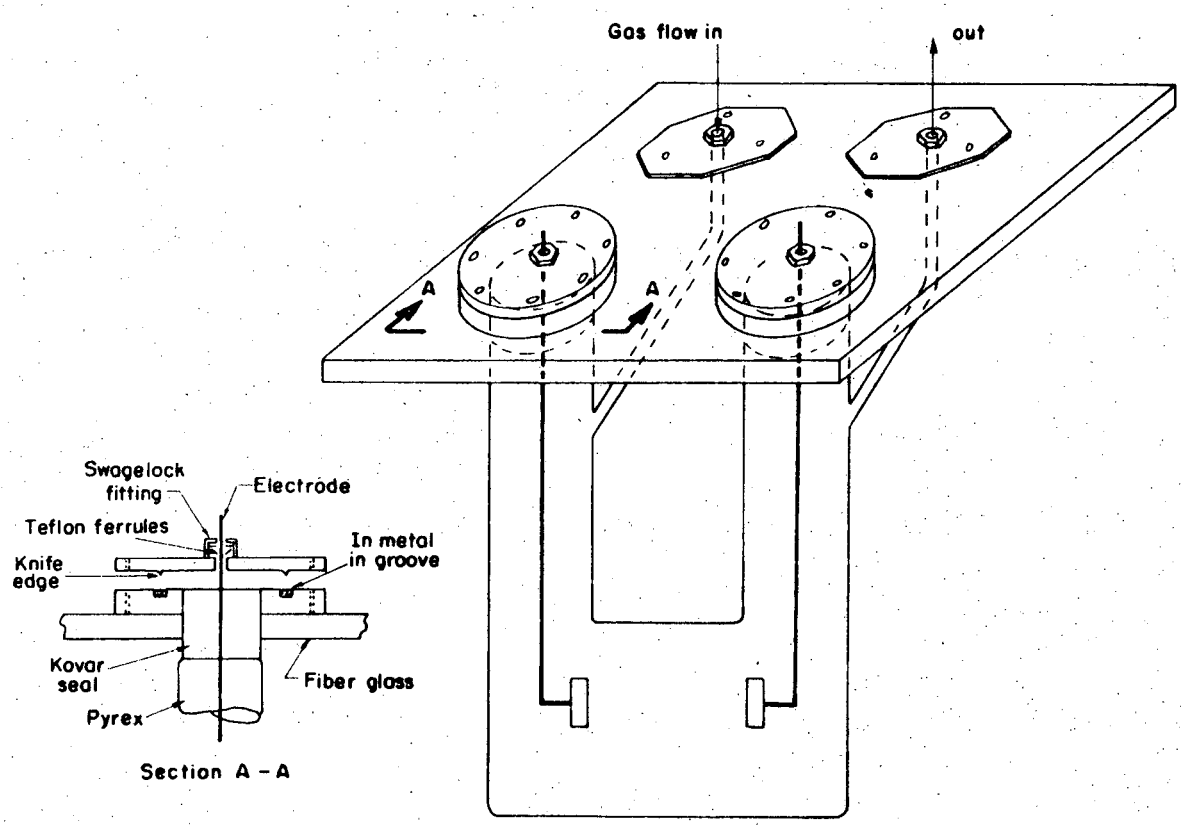


Figure VI-2 Electric discharge apparatus for $KrF_2$ preparation, with horizontal discharge and removable electrodes. Section A-A shows indium metal seal.

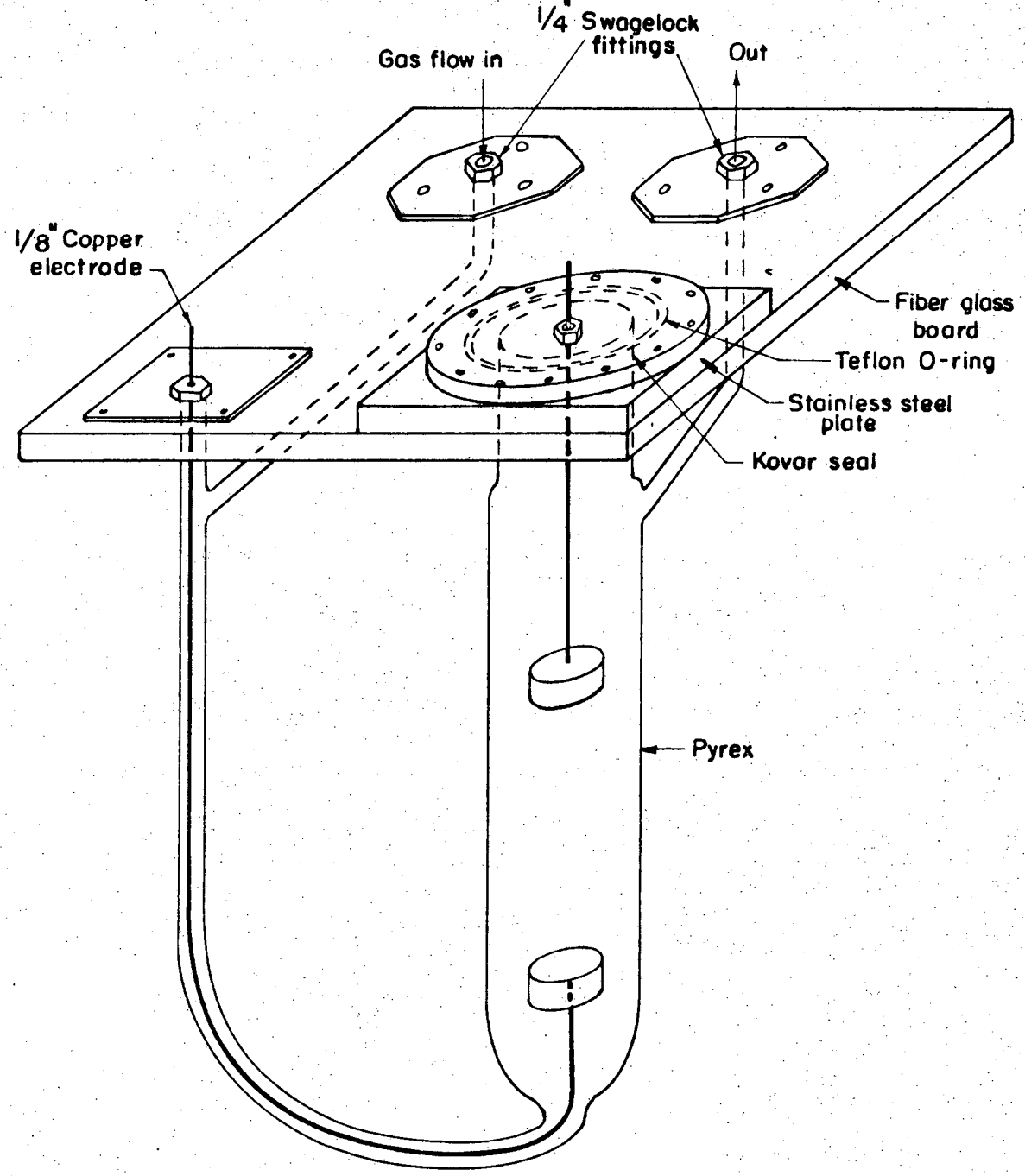


Figure VI-3 Electric discharge apparatus for $KrF_2$ preparation, with vertical discharge and removable electrodes. The upper electrode is sealed with teflon ferrules through the stainless steel plate, which is sealed to the Kovar with a 2" teflon O-ring. The lower electrode tip may be removed and replaced with tongs.

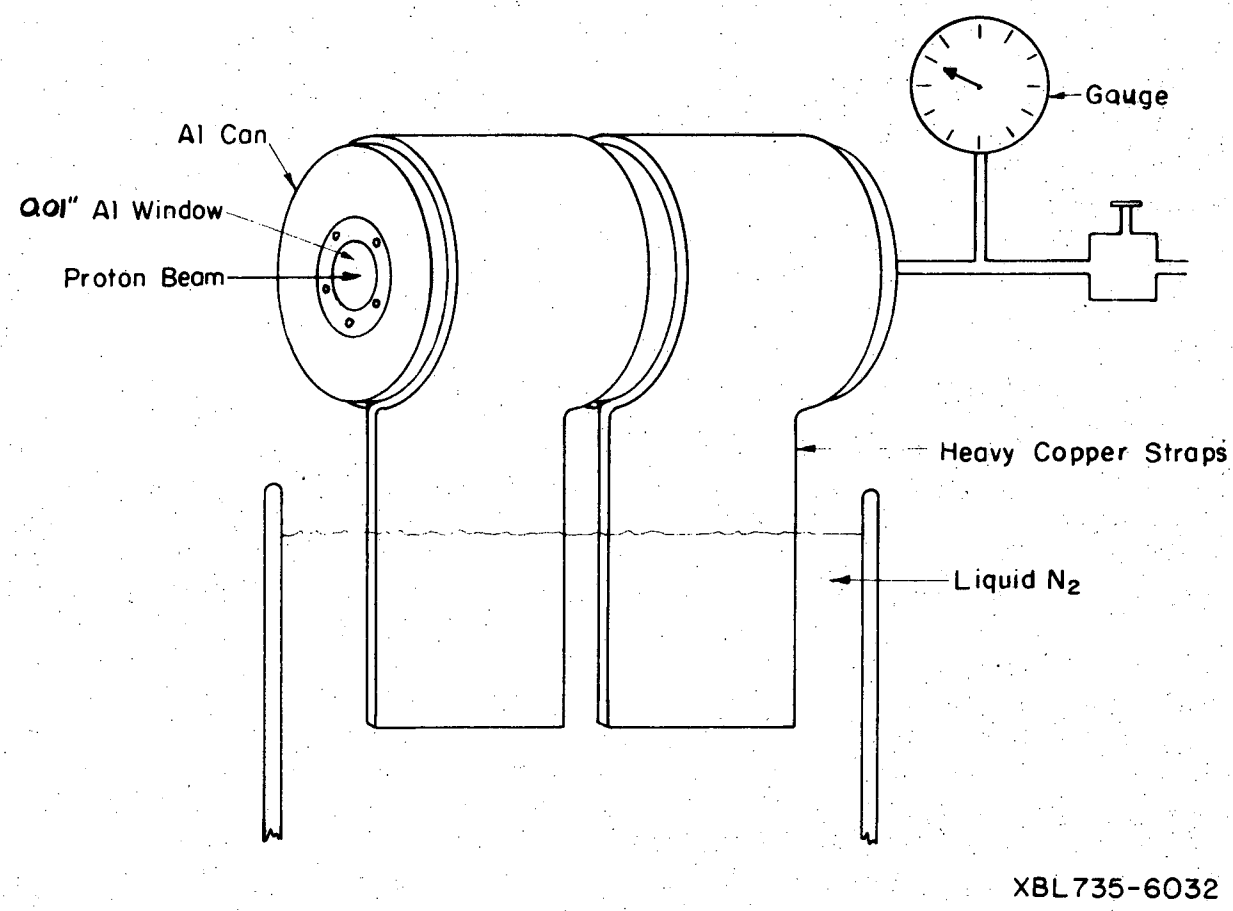


Figure VI-4 Proton bombardment apparatus for $KrF_2$ preparation.

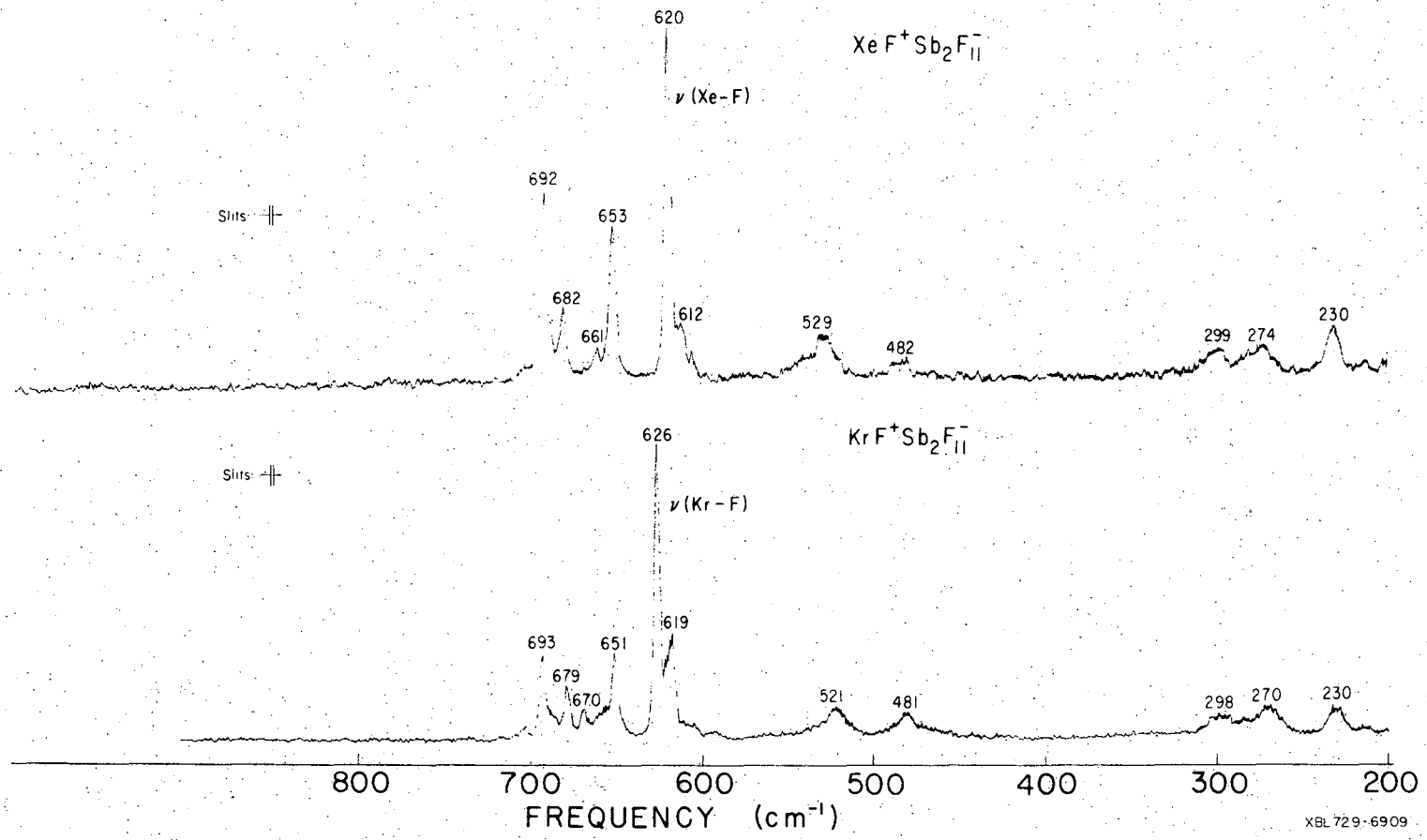


Figure VI-5 Raman spectra of $XeF^+Sb_2F_{11}^-$ and $KrF^+Sb_2F_{11}^-$

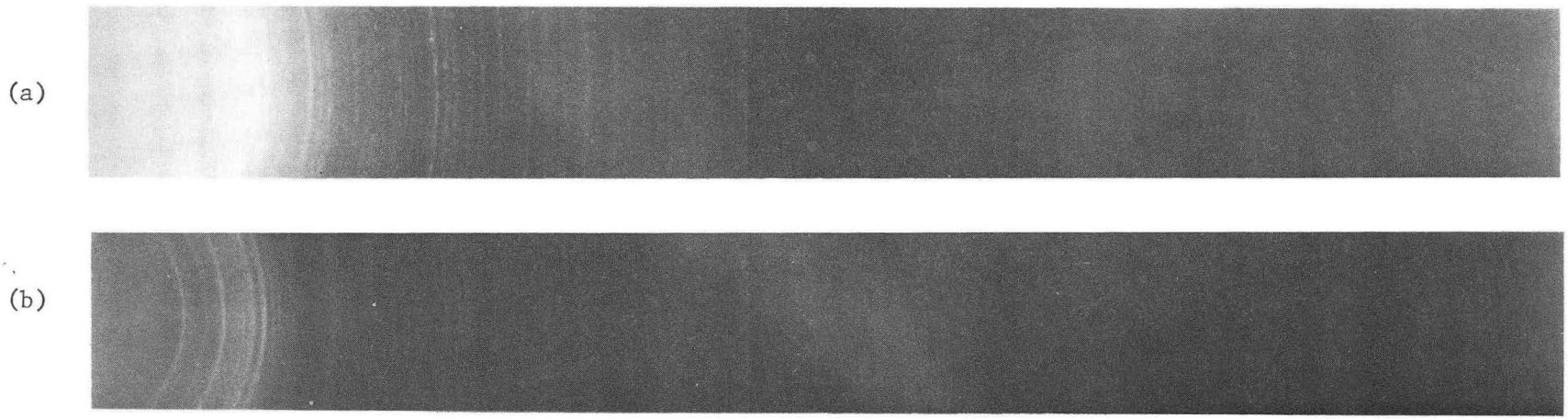


XBB 735-3139

Figure VI-6 X-ray powder diffraction patterns of (a) $XeF^{+}Sb_2F_{11}^{-}$ and (b) $KrF^{+}Sb_2F_{11}^{-}$. See Table VI-4 for a listing of the diffraction lines.

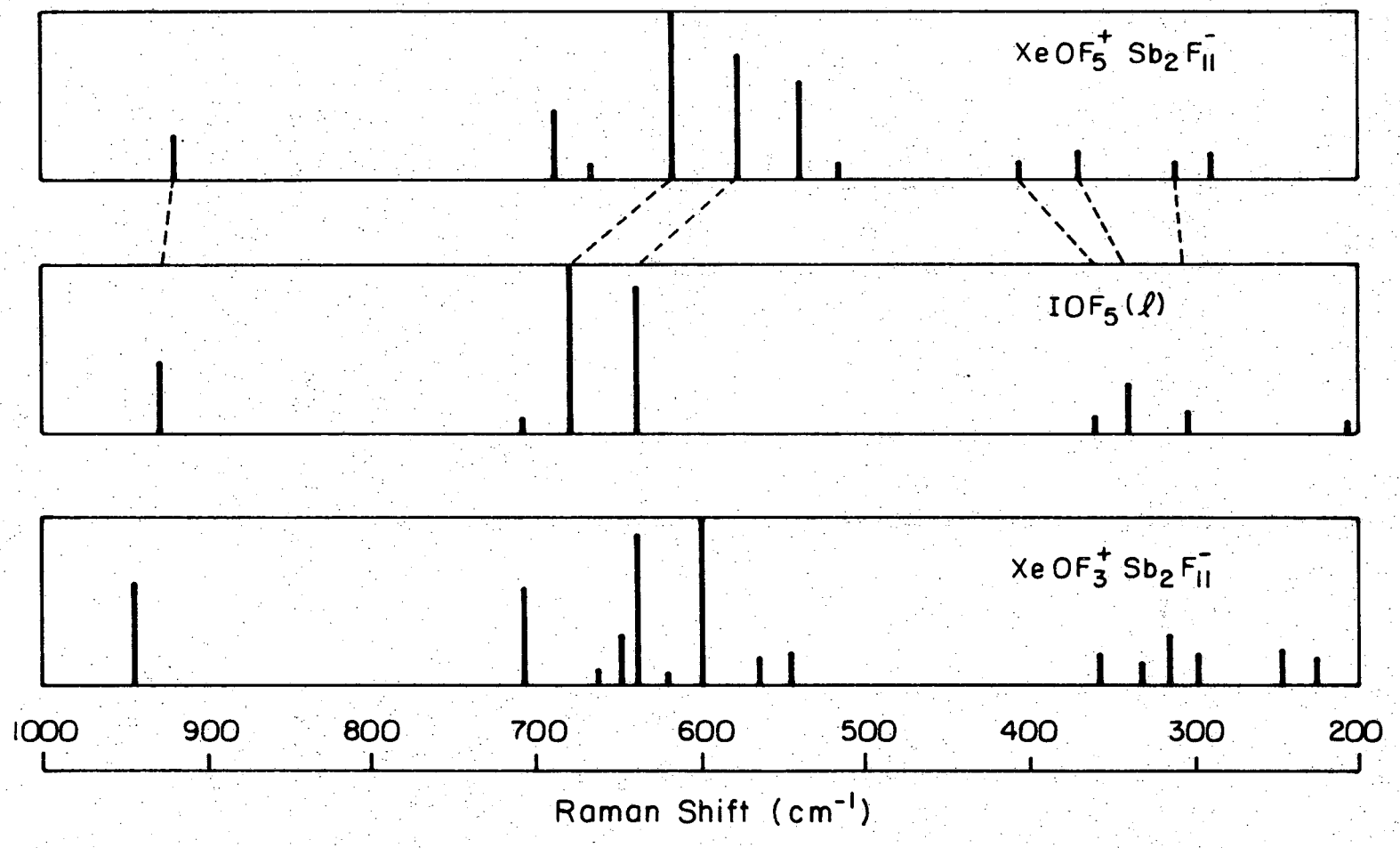


XBL 729-6984

Figure VI-7 Diagramatic Raman spectra of $XeOF_5^+Sb_2F_{11}^-$, $IOF_5$ (ref. 32), and $XeOF_3^+Sb_2F_{11}^-$.

Table VI-4

X-Ray Powder Data for $KrF^{+}Sb_2F_{11}^{-}$

| d Å | $10^4$ $1/d^2$ | $I/I_o$ |
|---|---|---|
| 5.844 | 293 | 7 |
| 5.651 | 312 | 1 |
| 5.052 | 392 | 4 |
| 4.550 | 482 | 9 |
| 4.095 | 596 | 2 |
| 3.897 | 658 | 8 (b) |
| 3.735 | 716 | 10 (b) |
| 3.560 | 788 | 3 |
| 3.478 | 827 | 3 |
| 3.277 | 931 | 2 |
| 2.928 | 1165 | 1 |
| 2.831 | 1247 | 2 (b) |
| 2.350 | 1811 | 4 |
| 2.257 | 1962 | 1 |
| 2.205 | 2057 | 2 (b) |
| 2.182 | 2099 | 1 |
| 2.088 | 2293 | 2 |
| 2.049 | 2382 | 5 |
| 1.991 | 2523 | 1 |
| 1.955 | 2615 | 3 (b) |
| 1.880 | 2827 | 1 |
| 1.831 | 2982 | 1 |
| 1.783 | 3145 | 2 |
| 1.740 | 3301 | 2 |
| 1.696 | 3474 | 2 |
| 1.661 | 3623 | 3 |

Table VI-4 (continued)

| d Å | $10^4$ $1/d^2$ | $I/I_o$ |
|---|---|---|
| 1.634 | 3744 | 1 |
| 1.596 | 3921 | 4 |
| 1.527 | 4283 | 2 |
| 1.496 | 4468 | 2 |
| 1.450 | 4756 | 3 |

Table VI-5

X-Ray Powder Data for $XeOF_5^+Sb_2F_{11}^-$

| d Å | $10^4$ $1/d^2$ | $I/I_o$ |
|---|---|---|
| 8.399 | 142 | 3 |
| 5.937 | 284 | 2 |
| 5.086 | 386 | 6 |
| 4.693 | 454 | 5 (vb) |
| 4.364 | 525 | 1 |
| 4.125 | 588 | 8 (b) |
| 3.937 | 645 | 10 (b) |
| 3.767 | 705 | 7 |
| 3.582 | 778 | 7 |
| 3.369 | 880 | 2 |
| 3.259 | 942 | 2 |
| 3.129 | 1021 | 5 |
| 2.910 | 1180 | 3 |
| 2.811 | 1266 | 1 |
| 2.744 | 1328 | 1 |
| 2.649 | 1424 | 3 |
| 2.534 | 1558 | 1 |
| 2.348 | 1814 | 4 |
| 2.299 | 1891 | 5 |
| 2.202 | 2060 | 5 |
| 2.141 | 2182 | 2 |
| 2.066 | 2341 | 4 |
| 2.021 | 2448 | 1 |
| 1.965 | 2590 | 1 |
| 1.882 | 2822 | 1 |
| 1.854 | 2911 | 1 |
| 1.823 | 3009 | 1 |

Table VI-5 (continued)

| d Å | $10^4$ $1/d^2$ | $I/I_o$ |
|---|---|---|
| 1.787 | 3130 | 3 |
| 1.743 | 3292 | 2 |
| 1.686 | 3518 | 3 |
| 1.642 | 3710 | 2 |
| 1.598 | 3916 | 3 |
| 1.561 | 4106 | 2 |
| 1.532 | 4258 | 2 |
| 1.422 | 4947 | 2 |
| 1.404 | 5075 | 1 |
| 1.353 | 5460 | 2 |

## REFERENCES


1. (a) S. P. Beaton, Ph.D. Thesis, University of British Columbia, Vancouver, 1966;
   (b) "The Manipulation of Air-Sensitive Compounds", D. F. Shriver, McGraw-Hill, 1969.
2. A. R. Young, II, T. Hirata, and S. I. Morrow, JACS, 86, 20 (1964).
3. N. Bartlett and D. H. Lohmann, Proc. Chem. Soc., 115 (1962).
4. J. Shamir and J. Binenboym, Inorg. Chim. Acta 2, 37 (1968).
5. J. B. Beal, Jr., C. Pupp, and W. E. White, Inorg. Chem. 8, 828 (1969).
6. Z. K. Nikitina and V. Ya. Rosolovskii, Izv. Akad. Nauk. SSSR, Ser. Khim., 2173 (1970).
7. J. Shamir, J. Binenboym, H. H. Claassen, JACS 90, 6223 (1968).
8. "International Tables for X-ray Crystallography," Vol. I, Kynoch Press, Birmingham, England, 1952.
9. J. A. Ibers and W. C. Hamilton, J. Chem. Phys. 44, 1748 (1966).
10. N. Bartlett and D. H. Lohmann, J. Chem. Soc., 619 (1964).
11. N. Bartlett and S. P. Beaton, Chem. Comm., 167 (1966).
12. D. E. McKee, R. Mews, and N. Bartlett, Abstracts of the 162nd ACS National Metting, Sept. 14-16, 1971, FLUO 2; N. Bartlett, D. Gibler, D. McKee, R. Mews, and M. Wechsberg, Abstracts of the Sixth International Symposium on Fluorine Chemistry, July 18-23, 1972, C24.
13. D. E. McKee, C. J. Adams, and N. Bartlett, Inorg. Chem., in press.
14. V. M. McRae, R. D. Peacock, and D. R. Russell, Chem. Comm., 62 (1969).

15. D. E. McKee, A. Zalkin, and N. Bartlett, Inorg. Chem., in press.

16. M. D. Lind and K. O. Christe, Inorg. Chem. 11, 608 (1972).

17. Azaroff and Buerger, "The Powder Method," McGraw-Hill Book Co., Toronto, 1958, p. 238.

18. N. Bartlett and F. O. Sladky, JACS, 90, 5316 (1968).

19. F. O. Sladky, P. A. Bulliner, N. Bartlett, B. G. DeBoer and A. Zalkin, Chem. Comm., 1048 (1968).

20. F. Hollander, Ph.D. Thesis, University of California, Berkeley, 1971.

21. N. Bartlett, M. Gennis, D. D. Gibler, B. K. Morrell and A. Zalkin, Inorg. Chem., in press.

22. N. Bartlett and N. K. Jha, unpublished observation, 1964.

23. D. Martin, C. R. Acad. Sci. Paris, C, 1145 (1969).

24. F. O. Sladky, P. A. Bulliner, and N. Bartlett, J. Chem. Soc. (A), 2179 (1964).

25. G. L. Gard and G. H. Cady, Inorg. Chem. 3, 1745 (1964).

26. H. Selig, Inorg. Chem. 5, 183 (1966).

27. R. J. Gillespie, B. Landa and G. J. Schrobilgen, Chem. Comm. 1543, (1971).

28. R. J. Gillespie, B. Landa and G. J. Schrobilgen, Chem. Comm., 607 (1972).

29. H. H. Claassen, H. Selig and J. G. Malm, JACS, 84, 3593 (1962).

30. C. L. Chernick, H. H. Claassen, J. G. Malm, and P. L. Plurien, "Noble Gas Compounds", H. H. Hyman, Ed., University of Chicago, Chicago, Illinois (1963).

31. I. Sheft, T. M. Spittler, and F. H. Martin, Science 145, 701 (1964).

32. G. M. Begun, W. H. Fletcher and D. F. Smith, J. Chem. Phys. 42, 2236 (1963).

33. A. A. Woolf and N. N. Greenwood, J. Chem. Soc., 2200 (1950).

34. H. Selig, H. H. Claassen, and J. H. Holloway, J. Chem. Phys. 52, 3517 (1970).

35. D. E. McKee, D. D. Gibler, C. J. Adams and N. Bartlett, to be published.

36. J. Martins and E. B. Wilson, Jr., J. Mol. Spectrosc. 26, 410 (1968).

37. K. Leary and N. Bartlett, Chem. Comm., 903 (1972); K. Leary, A. Zalkin and N. Bartlett, Chem. Comm., 131 (1973).

38. A. J. Edwards, personal communication with N. Bartlett.

39. N. Bartlett and M. Wechsberg, Z. anorg. allg. Chem., 385, 5 (1971).

40. G. R. Jones, R. D. Burbank, and N. Bartlett, Inorg. Chem. 9, 2264 (1971).

41. K. O. Christe, Inorg. Chem. 11, 1215 (1972).

42. D. D. Gibler, C. J. Adams, M. Fischer, A. Zalkin and N. Bartlett, Inorg. Chem. 11, 2325 (1972).

43. P. A. Doyle and P. S. Turner, Acta Cryst. A24, 390 (1968).

44. D. T. Cromer and D. Liberman, J. Chem. Phys. 53, 1891 (1970).

45. N. Bartlett, Endeavour, XXXI, 107 (1972).

46. R. J. Gillespie and R. S. Nyholm, Quart. Revs., XI, 339 (1957); R. J. Gillespie in "Noble-Gas Compounds", H. H. Hyman, ed., University of Chicago Press, Chicago and London, 1963, pp. 333-339.

47. D. F. Smith, J. Chem. Phys. 21, 609 (1953).

48. D. W. Magnuson, J. Chem. Phys. 27, 223 (1957).

49. B. K. Morrell, M.Sc. Thesis, University of California, Berkeley (1971).

50. N. Bartlett, B. DeBoer, F. Hollander, F. O. Sladky, D. Templeton, and A. Zalkin, Inorg. Chem., in press.

51. A. Zalkin, K. Leary, D. Templeton, and N. Bartlett, Inorg. Chem., in press.

52. N. Bartlett, F. Einstein, D. F. Stewart, and J. Trotter, J. Chem. Soc., A, 1190 (1967).

53. J. A. Ibers, and W. C. Hamilton, Science 139, 106 (1963); J. H. Burns, P. A. Agron, and H. A. Levy, ibid., 1208 (1963).

54. (a) G. C. Pimentel, J. Chem. Phys. 19, 446 (1951);
(b) R. E. Rundle, JACS 85, 112 (1963).

55. "Comprehensive Inorganic Chemistry", A. F. Trotman-Dickenson, Ed., Pergamon Press, 1973, Vol. I.

56. V. I. Pepekin, Y. A. Lebedev, and A. Y. Apin, Zh. Fiz. Khim. 43, 1564 (1969).

57. S. L. Miller, Proc. Natl. Acad. Sci. 47, 1515 (1961).

58. H. J. Svec and G. D. Flesch, Science 142, 954 (1963).

59. JANAF Thermochemical Data, The Dow Chemical Company, Midland, Michigan (1969).

60. N. Bartlett and F. O. Sladky, J. Chem. Soc. (A), 2188 (1969).

61. G. K. Johnson, J. G. Malm and W. N. Hubbard, J. Chem. Thermo. 4, 879 (1972).

62. J. Berkowitz, W. A. Chupka, P. M. Guyon, J. H. Holloway, and R. Spohn, J. Phys. Chem. 78, 1461 (1971).

63. J. J. Turner, and G. C. Pimentel, Science 140, 974 (1963).

64. S. R. Grunn, J. Phys. Chem. 71, 2934 (1967).

65. A. V. Grosse, A. D. Kirshenbaum, A. G. Streng, and L. V. Streng, Science 139, 1047 (1963).

66. H. Selig and R. D. Peacock, JACS 86, 3895 (1964).

67. W. E. Falconer, private communication.

68. D. R. MacKenzie and I. Fajer, Inorg. Chem. 5, 699 (1966).

69. B. Liu and H. F. Schaefer III, J. Chem. Phys. 55, 2369 (1971).

70. J. Berkowitz and W. A. Chupka, Chem. Phys. Lett. 7, 447 (1970).

71. (a) K. O. Christe and W. Sawodny, Inorg. Chem. 6, 1783 (1967).
(b) K. O. Christe, Inorg. Chem. 9, 2801 (1970).

72. D. D. Gibler, Ph.D. Thesis, Princeton University, 1973.

73. K. O. Christe, private communication.

74. J. Passmore, Ph.D. Thesis, University of British Columbia, Vancouver, 1967.

75. D. E. McKee, C. J. Adams, A. Zalkin, and N. Bartlett, Chem. Comm. 26, 32 (1973).

76. H. A. Carter and F. Aubke, Inorg. Chem. 10, 2296 (1971).

77. C. J. Adams and A. J. Downs, Spectrochim. Acta 28A, 1841 (1972).

ACKNOWLEDGEMENTS

My sincerest thanks go to Professor Neil Bartlett who taught me more than facts. I hope that I have learned his freshness of approach to research and his daring in conceiving the novel. He always let me work my way, which was certainly not always the way he would have preferred. But in so doing, he inspired me. His enthusiasm and excitement over new results encouraged me. I wanted to satisfy him and myself. In his subtle way, he made me want to work to find the answers. Rarely have I felt such motivation, and I am most thankful for my personal and professional association with this man.

Of all the students, professors, post-docs, technicians, and researchers who have helped me at Berkeley and the Lawrence Labs who are deserving of recognition here, I particularly want to thank Kevin Leary, my personal student, teacher, and friend. His presence made bearable and even enjoyable many otherwise miserable times.

I am thankful that California is such a beautiful place to live. It is impossible to imagine my graduate school experience occurring anywhere but here.

Finally, thanks to several friends whom it is best to leave unnamed. You know who you are.

This work was done under the auspices of the U. S. Atomic Energy Commission.

*TECHNICAL INFORMATION DIVISION*
*LAWRENCE BERKELEY LABORATORY*
*UNIVERSITY OF CALIFORNIA*
*BERKELEY, CALIFORNIA 94720*